N72-17159

DEVELOPMENT OF REVERSE
BIASED p-n JUNCTION ELECTRON EMISSION

P. Fowler
E. C. Muly

FINAL REPORT

Prepared Under Contract No.
NAS1-8223-3

NRC ::::: NATIONAL RESEARCH CORPORATION
A SUBSIDIARY OF CABOT CORPORATION
CAMBRIDGE, MASSACHUSETTS 02142

DEVELOPMENT OF REVERSE
BIASED p-n JUNCTION ELECTRON EMISSION

P. Fowler
E. C. Muly

FINAL REPORT

Prepared Under Contract No.
NAS1-8223-3

NATIONAL RESEARCH CORPORATION
(A Subsidiary of Cabot Corporation)
70 Memorial Drive
Cambridge, Massachusetts   02142

for

NATIONAL AERONAUTICS AND SPACE ADMINISTRATION

TABLE OF CONTENTS

LIST OF FIGURES

LIST OF TABLES

DEVELOPMENT OF REVERSE
BIASED p-n JUNCTION ELECTRON EMISSION

By
P. Fowler and E. C. Muly

SUMMARY

Under National Aeronautics and Space Administration
Contract No. NAS1-5347, Task 13 completed in 1968 and sub-
sequent in house efforts, a cold cathode emitter of hot
electrons for use as a source of electrons in vacuum gauges
and mass spectrometers was developed using standard Norton
electroluminescent silicon carbide p-n diodes operated
under reverse bias conditions. Continued development
including variations in the geometry of these emitters was
carried out here such that emitters with an emission
efficiency (emitted current/junction current) as high as
3×10^{-5} were obtained. Pulse measurements of the diode
characteristics were made and showed that higher efficiency
can be attained under pulse conditions probably due to
the resulting lower temperatures resulting from such operation
Deterioration of the emitters was observed due to ion bombard-
ment resulting from low vacuum conditions. Improvement of
the emission efficiency could be obtained by operation in
high vacuum ($p < 10^{-5}$ Torr) and no deterioration in emission
was noted under months of operation in ultrahigh vacuum.
Ion implantation of nitrogen ions into low impurity p-type
SiC was carried out in order to obtain large area emitters.
Problems in obtaining ohimic contact to the p material pre-
vented complete evaluation of the resulting diodes. A hypo-
thesis is developed that ion implantation into diamond
is a fruitful approach for obtaining higher hot electron
emission currents. A SiC emitter was used to initiate a dis-

charge in a Redhead magnetron gauge under pressure conditions for which it was otherwise non-starting. Experimental and theoretical plausibility proofs are given to shows that the present SiC diode emitters are not capable of linearizing a Redhead Magnetron discharge gauge due to the prohibative diode power requirements. It is suggested that the present diodes would have great utility in replacing the hot cathode of a Lafferty magnetron gauge.

2

DEVELOPMENT OF REVERSE
BIASED p-n JUNCTION ELECTRON EMITTER

By
P. Fowler and E. C. Muly
National Research Corporation
(A Subsidiary of Cabot Corporation)

INTRODUCTION

Under Task 13 of Contract NAS1-5347, a research and development program was carried out to produce a silicon carbide cold cathode electron emitter, for use as a source in ionization vacuum gauges and mass spectrometers. Because of the method used to yield the emission, namely the acceleration of electrons to higher energy states by applying a reverse bias to a SiC p-n junction, the electrons so emitted are termed hot electrons. Some investigations were made into the mechanism responsible for the hot electron emission and the electron emission efficiency $\left(\dfrac{\text{emitted current}}{\text{junction current}}\right)$ of many SiC p-n junctions were determined. The maximum emission efficiency determined during the program was 4×10^{-6} for an applied current of .06 A and an applied voltage of 23 volts.

Subsequent to that work, in house efforts were carried on for a year to further increase the efficiency of the standard Norton SiC electroluminescent diode as a reversed biased electron emitter. As a result, one Norton diode was prepared and tested that had an electron emission efficiency of 1.5×10^{-5} for an applied current of 0.04 A and applied voltage of 18.5 volts. Additionally because of improvements in fabrication and treatment of diodes, the fraction of them that yielded greater than 10^{-9} Amperes emission current was increased during this in house work to about 50%.

The goal of task 3 of Contract NAS1-8223 was to continue the research and development program on reverse biased p-n junction electron emitters to attain silicon carbide emitters with emission currents as high as 10^{-3} amperes. A secondary goal of the program is the adaptation of such emitters to magnetron discharge gauges to improve the striking and linearity characteristics of the gauges.

NATURE OF ELECTRON EMISSION FROM SiC

In the final report[1] of Task 13 of Contract No. NAS1-5347, Research and Development Program to Produce a Silicon Carbide Cold Cathode (Hot Electron) Emitter, two possible mechanisms were described that would lead to hot electron emission from semi-conductor p-n junctions, namely:

1.   Zener tunnelling

2.   Avalanche multiplications.

The former process is equivalent to internal field emission of the electrons and requires rather heavy doping levels in order the desirable potential conditions be established under reverse bias. The energy bands in such a case are indicated schematically in Figure 1. If the doping is sufficient for such extreme band bending to occur then (Zener) tunnelling from valence to conduction will occur.

The latter process of avalanche multiplication occurs when under increased reverse bias of the junction, electrons are accelerated within the crystal to high energies. If the energy is sufficient, the impact of these electrons with neutral

4
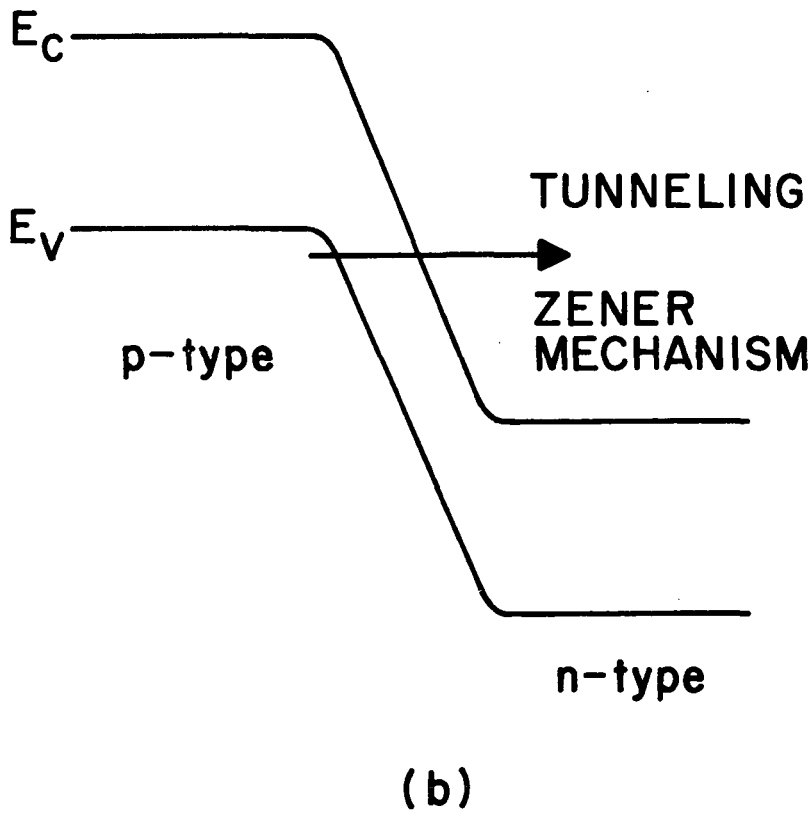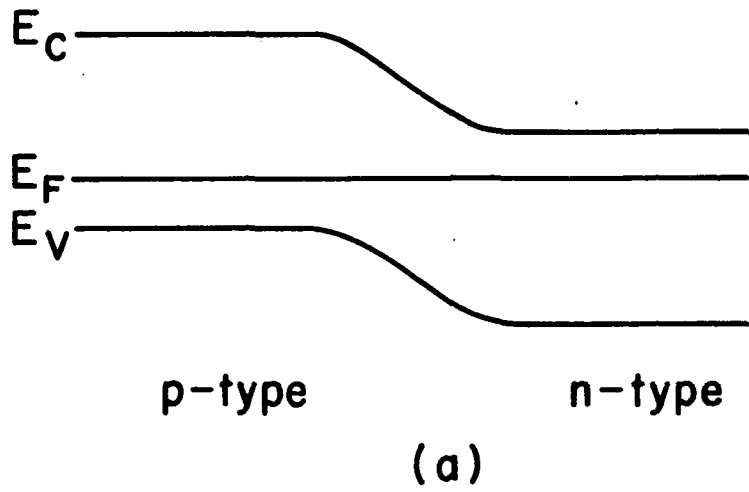
Figure 1. - Band Diagram for a Zener Diode with (a) No
Voltage Applied and (b) Reverse Bias.

atoms results in ionization and the conditions are favorable for an avalanche process with an electron-hole microplasma resulting. Since the temperature dependence of these two mechanisms is quite different it would be necessary to perform experiments to determine which mechanism is predominantly responsible for the emission in a manner such that temperature may be independently controlled.

Electron emission from reverse biased SiC p-n junctions has been experimentally investigated by numerous groups for at least 2 decades. Patrick and Choyke suggested in 1958[2] that the electron emission was probably from the same area that the blue light radiates from under reverse bias ("blue spots"). Since that time several groups (e.g., Stepanov[3], Brander[4]), have shown by electromagnetically focusing the electron emission onto a Willemite screen that, in fact, the electrons do originate from sites of "blue spots" and further that these are sites at which breakdown occurs and they are associated with defects in the SiC structure. Such sites can be generated by mechanically damaging the crystal by grinding (Brander[5]) or by picking (Greebe[6]). Suggestions made by Patrick or others that the sites are ones where free carbon particles or β-SiC exist in the α-SiC matrix have not been proved. As a proof that these "blue spots" are breakdown sites it is noted that in order to attain "harder"

reverse characteristics with higher breakdown voltages in SiC and SiC p-n junction devices the etching away of "blue spots" is carried out. It is generally assumed that these breakdown sites are hot electron-hole microplasmas. Brander's [7] analysis shows the microplasma temperature to be about 6800°K. The radiation from these areas is shown by Patrick[8] to have a 4.6 eV maximum to its spectrum. This is $\frac{3}{2}$ the SiC energy gap and suggests that the origin of the light is from impact ionization. This energy is greater than the electron affinity of about 4 eV and thus could make possible emission of hot electrons. Stepanov, et al[3] also present evident that impact ionization of impurity centers by fast electrons is the concept behind reverse currents and the blue spot radiation.

In the present investigation an extreme example of such a breakdown region was observed. The inside surface of a tubelike void included within the crystal was noted at a particular reverse bias to light up with blue light in a similar manner to the starting of a fluorescent lamp discharge. At that precise voltage a change in slope of the reverse characteristic was noted and is shown in Figure 2. The void, which appeared to have some excess black material (carbon?) on its inner surface was sufficiently far inside the crystal that any hot electrons that may have been generated could not reach the outside and be collected. Under large enough reverse bias the increased current flow at this breakdown site was sufficient to yield incipient white light generation and finally enough power was dissipated at the junction that catastrophic, irreversible breakdown of the junction resulted.

7
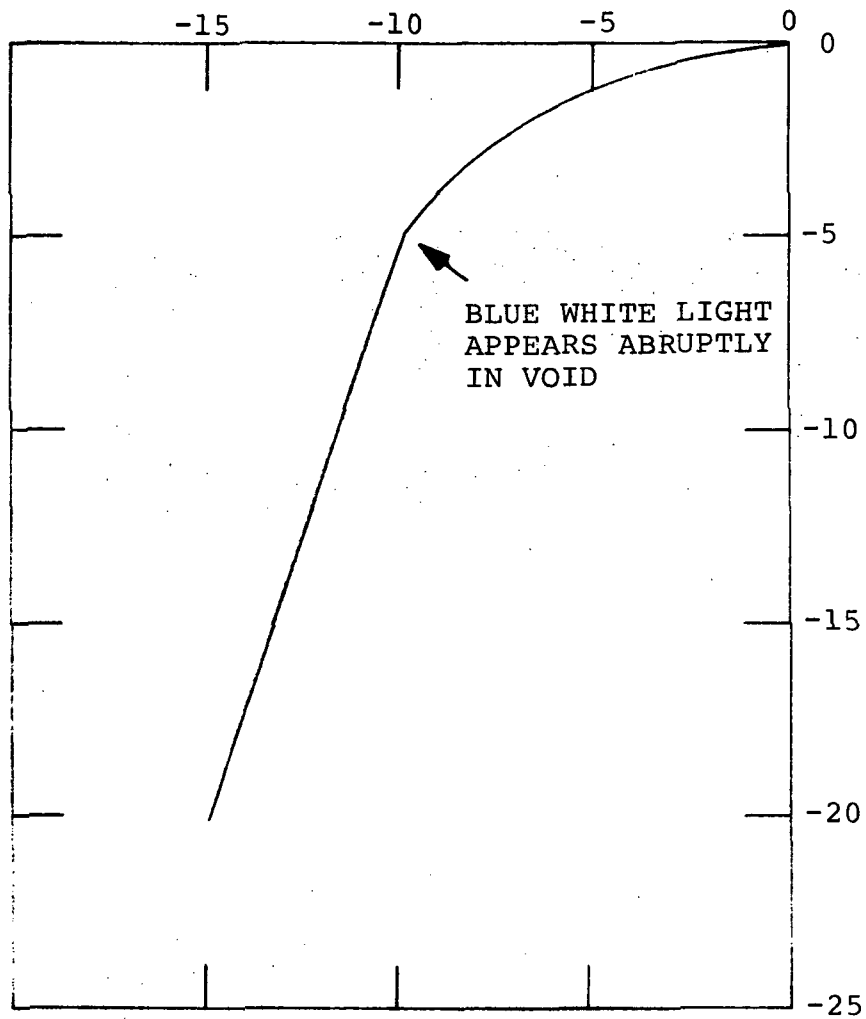
Figure 2. - Reverse Current Characteristic
for SiC Crystal with Void Included
in Bulk.

8

The fact that a specific site may have such a large effect on the reverse current suggests the demise of a scheme which hopes to take advantage of uniform emission over large areas since it implies that the presence of one such breakdown site will lead to the effect that nearly all the reverse current will "short circuit" through such a point and the remaining junction area will minimally be involved in the reverse current flow and resulting hot electron emission in opposition to the suggestions of Hodgkinson[9].

EXPERIMENTAL

Electron Emission

It was earlier mentioned that independent control of the temperature is required in the experimental investigation to determine the mechanism for electron emission. As an example of the problems encountered heretofore in this respect, the power input to and output from a crystal during a typical electron emission experiment can be compared. For a 2 mm x 2 mm x 0.1 mm SiC crystal mounted in 20% Be-Cu electrodes, in vacuum, having 20 V applied across its faces, the current flow would be approximately 0.05 A to obtain reasonable electron emission. If one assumes that the 1 watt of power generated is entirely dissipated by means of radiation with an emissivity E, of unity then the temperature, T, attained by the device may be obtained by equating power input, P, to the power radiation balance at the surface of the crystal in the steady state:

$$P = 1 \, wt = \sigma \, \varepsilon \, A \, (T^4 - T_o^4) \qquad (1)$$

where σ is the Stefan-Boltzmann constant, T_o is the environmental temperature, and A is the total area of the device. For the crystal described above the temperature thus calculated would be $\sim 900°C$.

Such a temperature would lead to violation of the assumption of radiative cooling alone, conduction to nearby crystal holder parts becoming a predominant heat loss mechanism. However, even with the largest standard Norton SiC crystal heat sink, an example of which is shown in Figure 3, the crystal temperature increase under the dc conditions required for obtaining useful electron emission (~ 1 watt) can be calculated to be as much as $300°C$. Thus, dc measurement of electron emission under isothermal conditions is not possible.

In order to limit the crystal temperature so that it could be independently controlled while not simultaneously limiting the instantaneous power level required for emission, pulsed operated was resorted to. Short duty cycles were used to limit the average power so that the crystal temperature rise was small.

The circuit shown in Figure 4 was constructed to provide the required pulses. Duty cycles as short as 2×10^{-4} were provided for with pulse durations ranging from 350 μ sec sec to 9 m sec. Independent variation of the applied junction voltage and the extraction voltage was provided for in order that the saturation characteristics of the emission could be studied. This latter provision allows one indirectly to de-
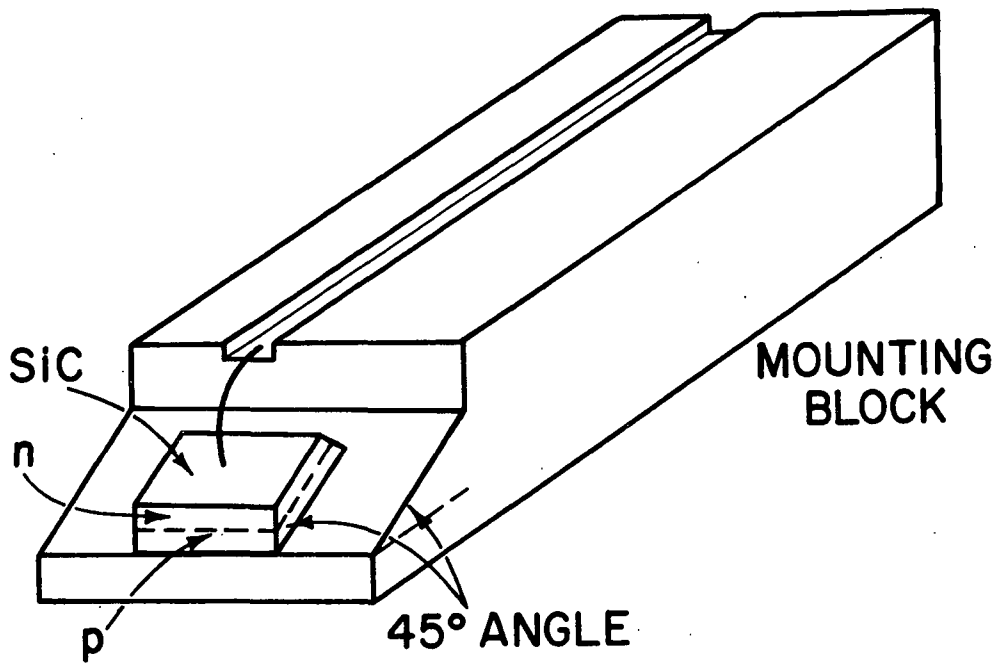
Figure 3. - SiC p-n Junction Mounted on Norton Heat Sink.
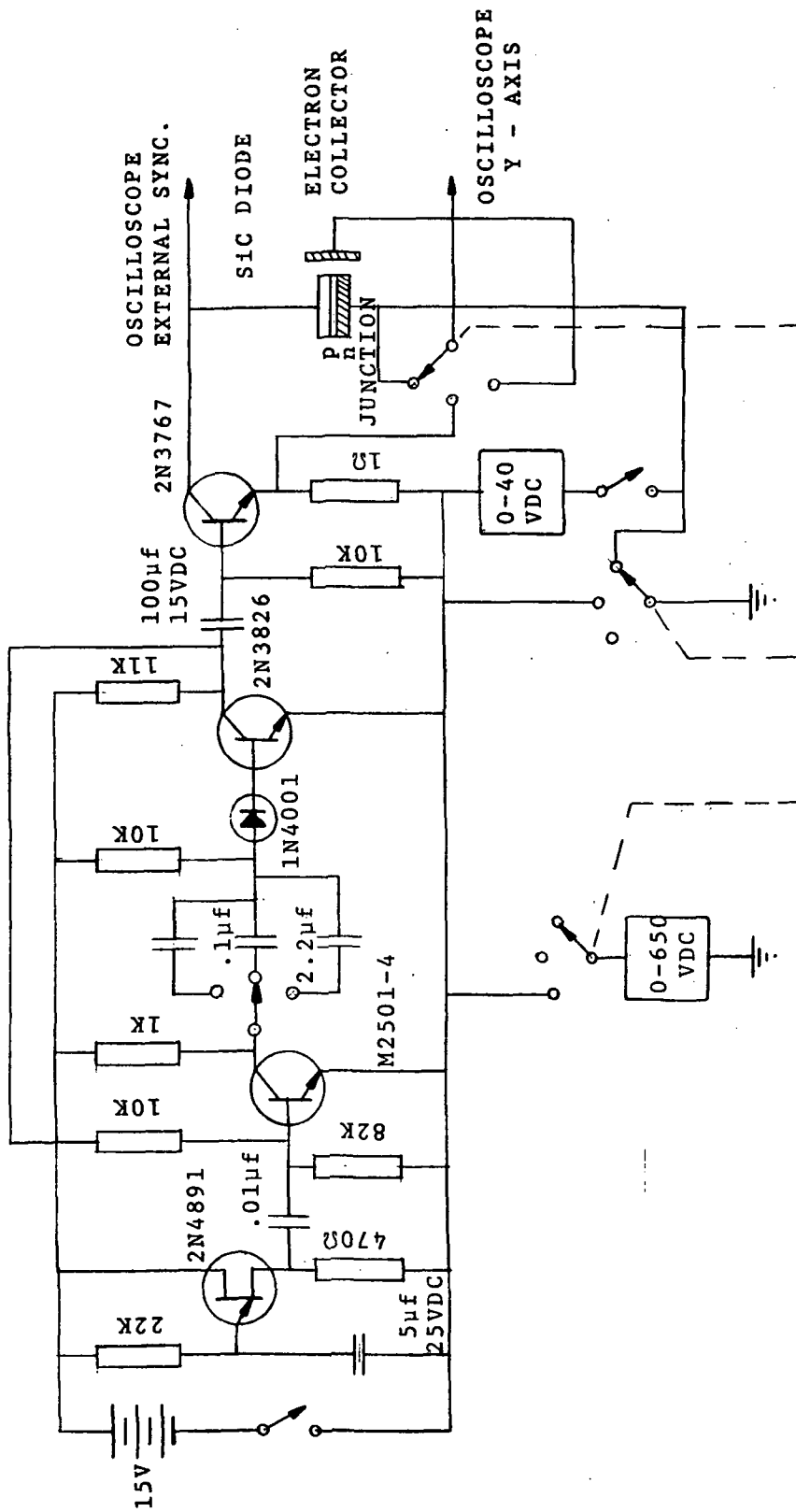
Figure 4. - Schematic of Junction Current Pulse Circuit

rive information about the geometry of the emitting region. The emitted electrons find themselves under the action of both the field of the junction which acts to draw them back into the n side of the crystal and the field of the extraction potential.

All diodes investigated were mounted in an oil diffusion pumped vacuum bell jar system. The diode was biased 650 volts negative with respect to the collector, the tip of a wire which was connected either to a Keithley 610 BR electrometer operated in the "fast" mode for dc measurements or to a Tektronix Model 545B Oscilloscope using a type w amplifier for pulsed mode measurements. The smallest signal that could be reliably measured in the pulsed mode of operation is limited by pick-up of random outside interferring noise and junction current pick-up capacitively coupled to the collector signal in a coherent manner. In the case of the system of Figure 4 the minimum measureable signal voltage level is 1 mV and the Type w amplifier input impedence is 1 megohm so that the minimum measureable collected emission current is 10^{-9} amperes. In order to obtain reasonable accuracy p-n junctions emitting currents two orders of magnitude greater than this minimum (10^{-7} amperes) must be collected. Since the average junction emission current is much less than this, only exceptional crystals may be used in emission measurements carried out under isothermal conditions. Figure 5 is a tracing of the oscilloscope display of the emission current from diode
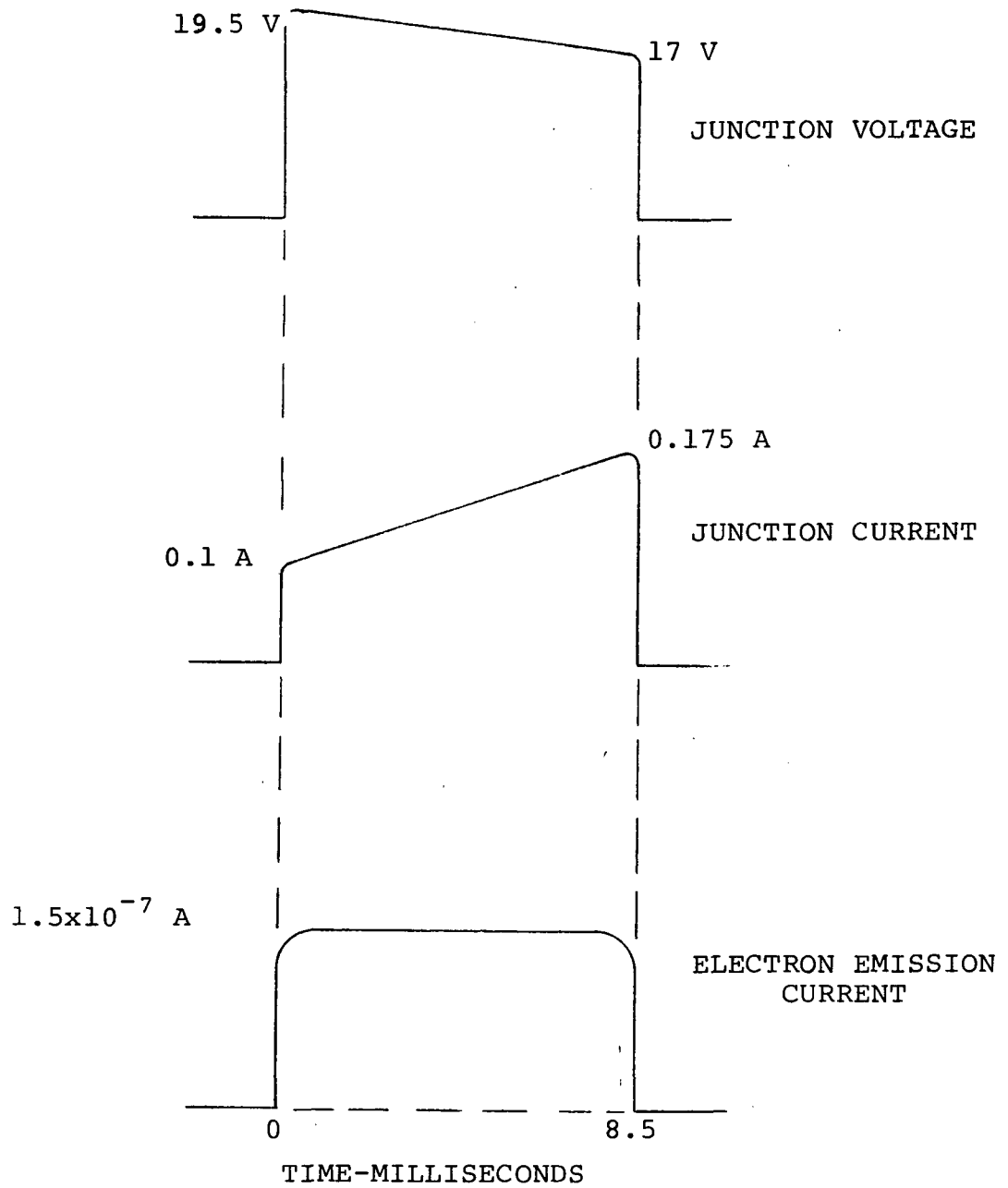
Figure 5. - Junction Voltage and Current and Emission
Current Under Pulse Conditions (0.7 pps).

14

2759-9-30-1 pulsed with a nearly rectangular pulse of 18
volts amplitude, 8.5 milliseconds long with a repetition rate
of 0.7 pps. Due to the relatively low thermal conductivity
of the SiC crystal there was an accompanying increase of
junction current from 0.1 A to 0.175 A during the application
of the pulse as is also shown in the figure. It may be noted
that this requires an accompanying decrease in quantum efficiency
or ratio of emission current to junction current with increasing
temperature. This is in agreement with the observations of
others[3].

It is noted in all investigations that a gradual decay
of electron emission occurs with time of operation. This has
been particularly so in our investigation whereby almost all
emitters measured have ultimately decayed to emission current
levels yielding them no longer useful ($< 10^{-9}$ A). Associated
with this decay is, invariably, a decrease in junction forward
and reverse I-V characteristics. As an example, initially a
measurement may indicate a reverse resistance for small applied
voltages of 200,000 Ω and a forward resistance of 10,000 Ω.
After an hour of operation of the diode at 30 V and .03 A
yielding a collected emission current of 2 x 10^{-9} A, both the
forward and reverse resistance of the junction are drastically
reduced to 1000 Ω or less.

An exception to the above behavior was diode 3059-63-A3.
This device, after being culled from a group of similar diodes
in a preliminary measurement of emission current in the normal
oil diffusion pumped system, was mounted in an ion pumped
system and after outgassing at 140°C overnight pressures in
the 10^{-8} Torr range were attained. This device after operating

at 50 mA junction current for several hours yielded emission currents as high as 8×10^{-7} A, even though such emission had not been obtained after the same treatment in the lower vacuum system. With that junction current the crystal heated up considerably above room temperature, possibly as high as 200°C although no temperature measurements were made. Brander and others have noted the necessity for such pretreatment at increased temperatures required in order to initiate substantial emission current levels. After such treatment the emission current remained constant during continual use of the junction. The diode was operated with no degradation for more than a month. However, when the ambient gas density was increased to greater than 10^{-4} Torr a gradual deterioration of emission current was observed although high emission was again restored in UHV.

The deterioration of emitters has been noted by Brander and Todkill[12] and by Windsor[10] to be a strong function of the ambient pressure, decay of the emission current being negligible at pressures of 10^{-9} Torr and less. Brander and Todkill ascribe the majority of the deterioration to the bombardment of the cathode by positive ions, the intensity of which will vary in proportion to the ambient gas density. The observations on diode 3059-63-A3 in this investigation supports this hypothesis and probably such cathode bombardment accounts for deterioration of all other emitters tested in the bell jar system in which the local pressures in the vicinity of the diode junction could have been greater than the nominal value of $\simeq 10^{-5}$ Torr at the ion gauge position near the throat of the diffusion pump.

Table I is a list of the SiC p-n junctions that were investigated for electron emission during the contract period.

I-V Characteristics

In addition to investigation of the relation of emission current to junction current, some understanding of the mechanism for emission can be derived from the relation of applied reverse junction voltage bias and resulting junction current and its variation with temperature. The normal electronic curve tracers which display such characteristics use a duty cycle on the order of 50% which is shown above to be inconsistent with the requirement of constant device temperature. An example of the measured characteristic of a reverse-biased SiC p-n junction mounted on a relatively massive heat sink is displayed in Figure 6. The dotted curve is the characteristic for pulse operation indicating breakdown via avalanche multiplication. The solid dc characteristic, shows the distortion that results from heating of the junction. The proposed solution to the problem of heating was, again, to provide for a greatly decreased duty cycle for the curve tracer. The circuit of Figure 7 was constructed in order to provide 100 V pulses with duty cycles as small as 10^{-6} if required.

TABLE I

SUMMARY OF   p-n   JUNCTION ELECTRON EMISSION MEASUREMENTS

DEVICE NUMBER	CONFIGURATION	DC OPERATION		PULSE OPERATION	
		MAXIMUM ELECTRON EMISSION(A)	MAXIMUM EMISSION EFFICIENCY	MAXIMUM ELECTRON EMISSION(A)	MAXIMUM EMISSION EFFICIENCY
TO-56-A	90° cleaved			3×10^{-8}	4×10^{-7}
TO-56-C	90° cleaved			0	0
TO-56-I	90° cleaved			1.6×10^{-9}	8×10^{-7}
TO-56-P	90° cleaved			4×10^{-9}	4×10^{-8}
TO-56-Q	90° cleaved			1.3×10^{-7}	1.2×10^{-6}
TO-56-1	90° cleaved			0	0
TO-56-2	90° cleaved			0	0
TO-56-3	90° cleaved	3.5×10^{-7}	1.2×10^{-5}	6.5×10^{-7}	$9. \times 10^{-6}$
TO-56-4	90° cleaved	1.7×10^{-10}	4.7×10^{-9}		
TO-56-5	90° cleaved	1.6×10^{-10}	2.2×10^{-9}		
TO-56-6	90° cleaved	0	0		
TO-56-7	90° cleaved	6×10^{-11}	4×10^{-9}		
TO-56-8	90° cleaved	2.4×10^{-9}	6×10^{-8}		
TO-56-9	90° cleaved				
TO-56-10	90° cleaved	2.6×10^{-10}	7.4×10^{-9}		
TO-56-11	90° cleaved	1.1×10^{-7}	7.3×10^{-6}	4×10^{-9}	2×10^{-9}
TO-56-12	90° cleaved	1.8×10^{-9}	9×10^{-8}		
TO-56-13	90° cleaved	0	0		
TO-56-14	90° cleaved	3			
NRC-1	90° unmounted	6.9×10^{-11}	6.9×10^{-9}		
NORTON-G	90° unmounted	1×10^{-11}	1.6×10^{-10}		
1001		8×10^{-11}	8×10^{-9}		
1263-B4A		1.85×10^{-8}	8×10^{-7}	1.5×10^{-9}	4×10^{-8}
2NR-A2	45° unmounted	1.2×10^{-9}	4×10^{-8}	0	0
2NR-A4	45° unmounted	1.6×10^{-11}	1.6×10^{-9}		

$\mathcal{D}$

TABLE I (Cont'd)

DEVICE NUMBER	CONFIGURATION	DC OPERATION		PULSE OPERATION	
		MAXIMUM ELECTRON EMISSION(A)	MAXIMUM EMISSION EFFICIENCY	MAXIMUM ELECTRON EMISSION(A)	MAXIMUM EMISSION EFFICIENCY
C207 2-13-1	15°unmounted	4.5×10^{-9}	1.5×10^{-7}		
C207 2-13-2	15°unmounted	6.5×10^{-9}	6×10^{-7}	1.5×10^{-6}	10^{-5}
C207 2-13-3	15°unmounted	2.2×10^{-5}		2×10^{-5}	3×10^{-5}
C207 2-17-70				0	0
2LER-A1	Multifaceted			0	0
2579 9-21-1				0	0
2579 9-21-2				0	0
2579 9-21-3				0	0
2579 9-21-4				0	0
2579 9-301	15°on heat sink	0	0		
2579 9-30-2	15°on heat sink	7×10^{-11}	3.1×10^{-9}		
2579 9-30-3	15°on heat sink	9×10^{-11}	1.6×10^{-9}		
2579 9-304	15°on heat sink	2×10^{-11}	4×10^{-10}		
2892 - 3C				0	0
28-ER-A1-1				2×10^{-6}	3×10^{-6}
2951-55-A3	45°on heat sink			0	0
2951-55-A4				0	0
2966-70A2	45°unmounted	3×10^{-9}	8×10^{-8}	2×10^{-7}	6×10^{-7}
2966-70-A9		5×10^{-10}	3×10^{-9}	$8 \times 10^{-}$	
3059-63-A1	90°on heat sink			0	0
3059-63-A3		7.7×10^{-7}	2.3×10^{-5}		
3059-63-A4		6.4×10^{-9}	$1. \times 10^{-7}$		
3059-63-A5		2.5×10^{-9}	4×10^{-8}	5×10^{-9}	4×10^{-8}
3084-87 A22		8.5×10^{-9}		2.2×10^{-6}	4×10^{-8}
32-ER-A3		2×10^{-11}	7×10^{-10}	5×10^{-8}	10^{-6}
32-ER-A4					
37-2					
4006-4010-A1					
4011-15-A2					

TABLE I (Cont'd)

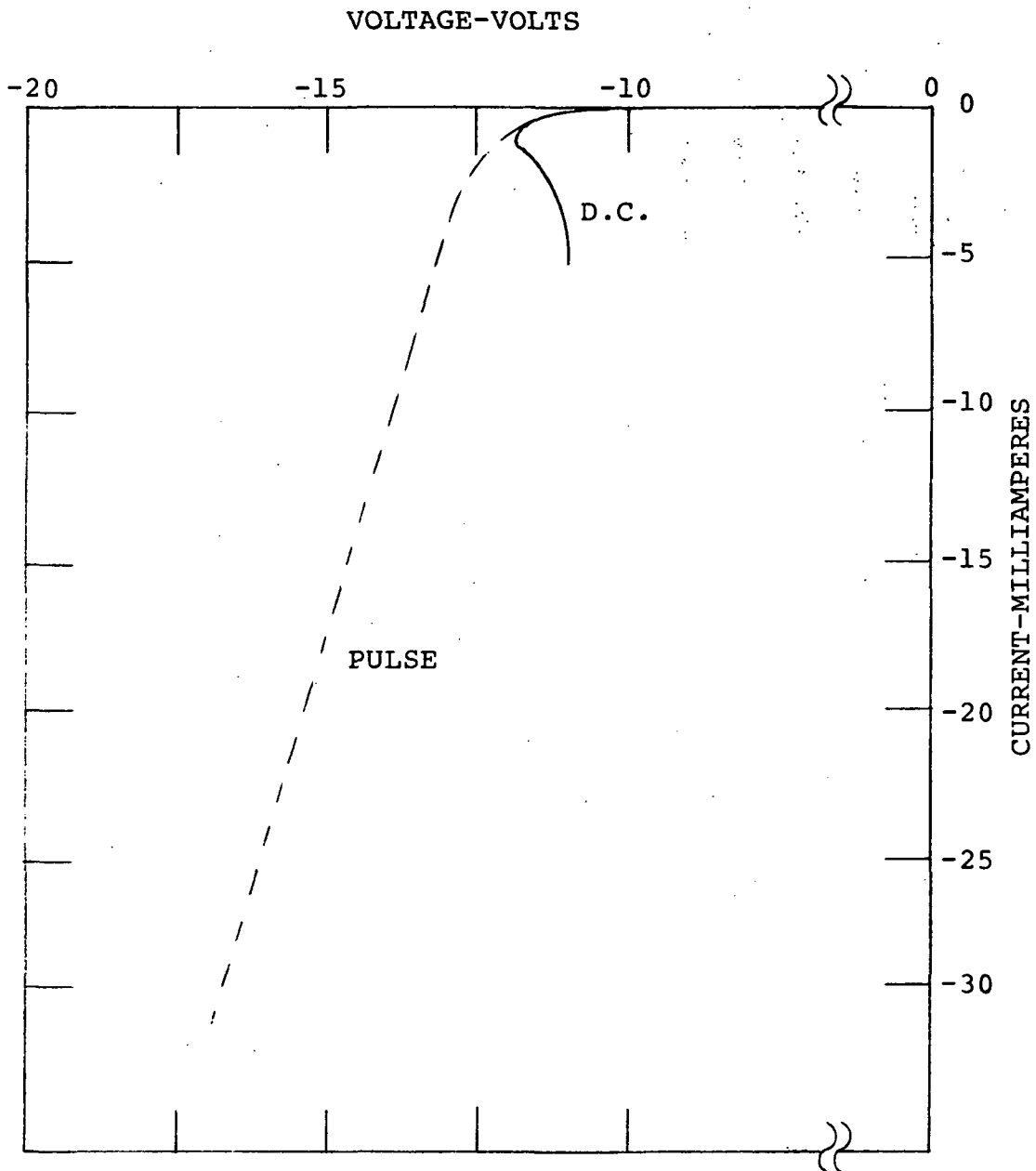| DEVICE NUMBER	CONFIGURATION	DC OPERATION		PULSE OPERATION	
		MAXIMUM ELECTRON EMISSION (A)	MAXIMUM EMISSION EFFICIENCY	MAXIMUM ELECTRON EMISSION (A)	MAXIMUM EMISSION EFFICIENCY
A1-4971					
53-ER		4×10^{-10}	8×10^{-9}	10^{-9}	3×10^{-8}
57-ER					
64-ER		0	0		
7514	PNP-no contacts				
C-82					
C-96-1					
C-96-2				10^{-6}	1.1×10^{-6}
C-96-3				0	0
82169-A28	90° unmounted	3.8×10^{-12}	7.6×10^{-9}		
6-8-70-1					
6-8-70-2					
6-8-70-3				10^{-6}	3.5×10^{-6}
7-13-70-A4				7.5×10^{-9}	4×10^{-8}
7-13-70-A5				5×10^{-6}	10^{-5}
7-13-70-A6				0	0

Figure 6. - Pulse and Direct Current IV Characteristics
of Diode 1263-B4 Illustrating the Influence
of Diode Temperature Rise.

180 VDC

10K

2N3739

JUNCTION

N   P

SiC DIODE

OSCILLOSCOPE
135 V, SAW-
TOOTH VOLTAGE
OUTPUT

470 Ω

1 Ω

2N2160

100K

B₂

E

B₁
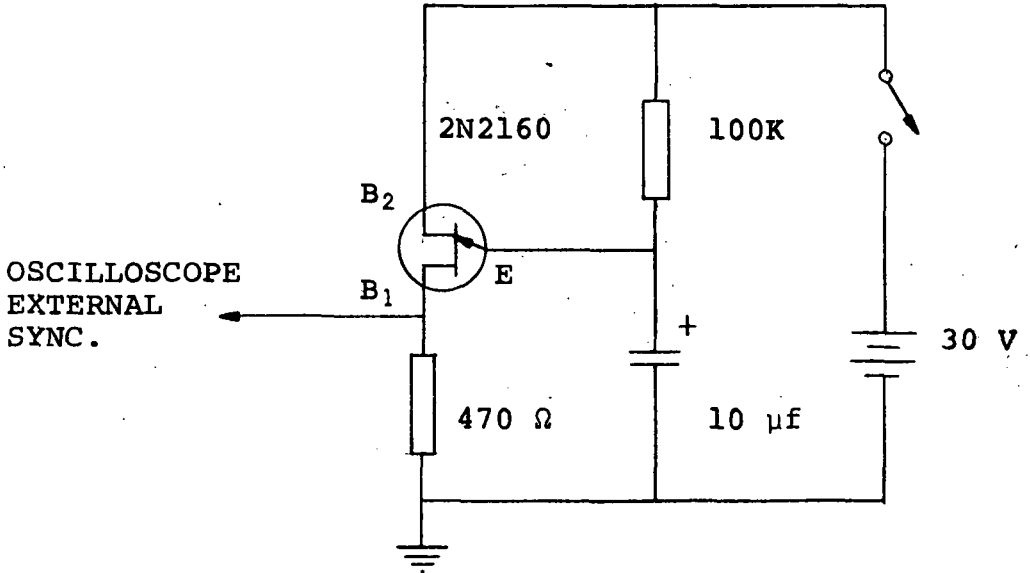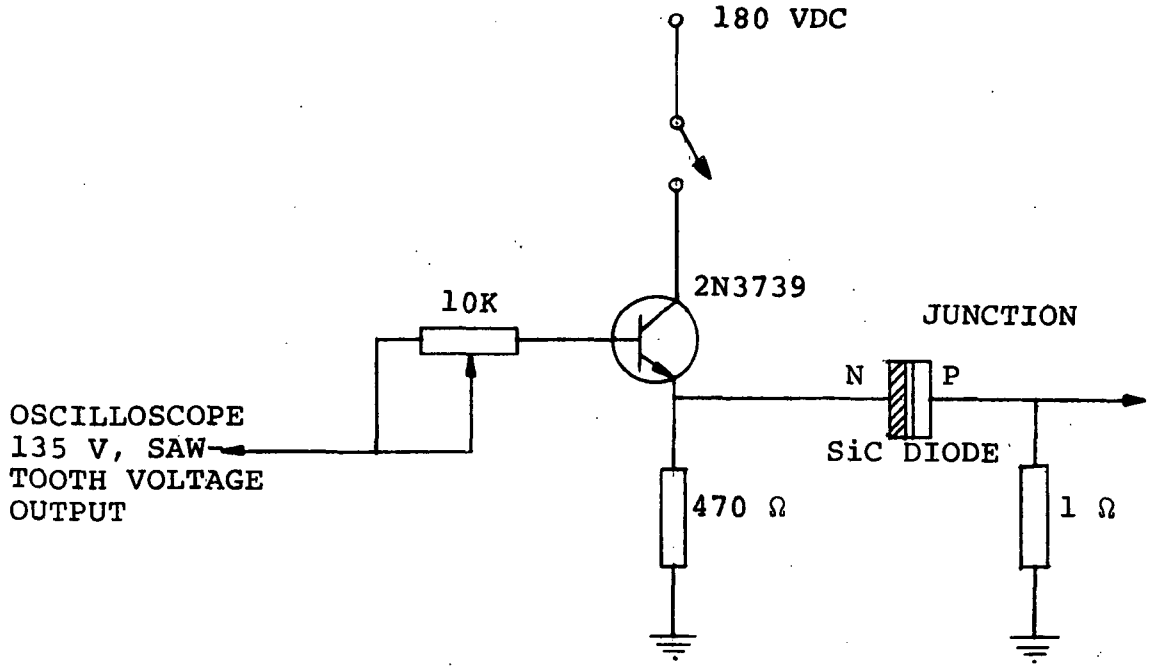
OSCILLOSCOPE
EXTERNAL
SYNC.

+

30 V

470 Ω

10 μf

Figure 7. - Schematic of Diode Curve Tracer.

Cesium Deposition. - An additional benefit from maintaining the crystal temperature relatively low may be gained in the investigation of increased electron emission resulting from cesium metal deposition which lowers the SiC work function. The serious nature of the experimental problem of cesium deposition becomes evident if one refers to Figure 8 which is a plot of the number of monolayers per second of cesium which will evaporate from a cesium surface as a function of surface temperature where a good sink for the evaporant is provided. It is seen that the lifetime of a cesiated surface maintained at room temperature is about 2 seconds which is too short for meaningful emission measurement to be carried out. This partially explains the reason for generally negative results obtained in the cesium deposition experiments performed on contract NAS1-5347, Task 13. In order that sufficient time be available for the measurement, Figure 8 indicates that the junction surface temperature must be maintained below 0°C. This is only possible under pulse conditions.

The alternative for obtaining a cesium surface is to introduce sufficient cesium into a sealed off system that an equilibrium vapor pressure equivalent to monolayer coverage ($\sim 5 \times 10^{-4}$ Torr) be maintained. Because of the possibility of shorting of the p-n junction due to excess cesium and because of the determintal reactive effect of an equilibrium vapor of cesium within the vacuum system this alternative was not pursued. Figure 9 is a schematic of the cesium vapor deposition system that was constructed. Provisions were made to measure and to separate out electron photoemission current from hot electron p-n junction electron emission.
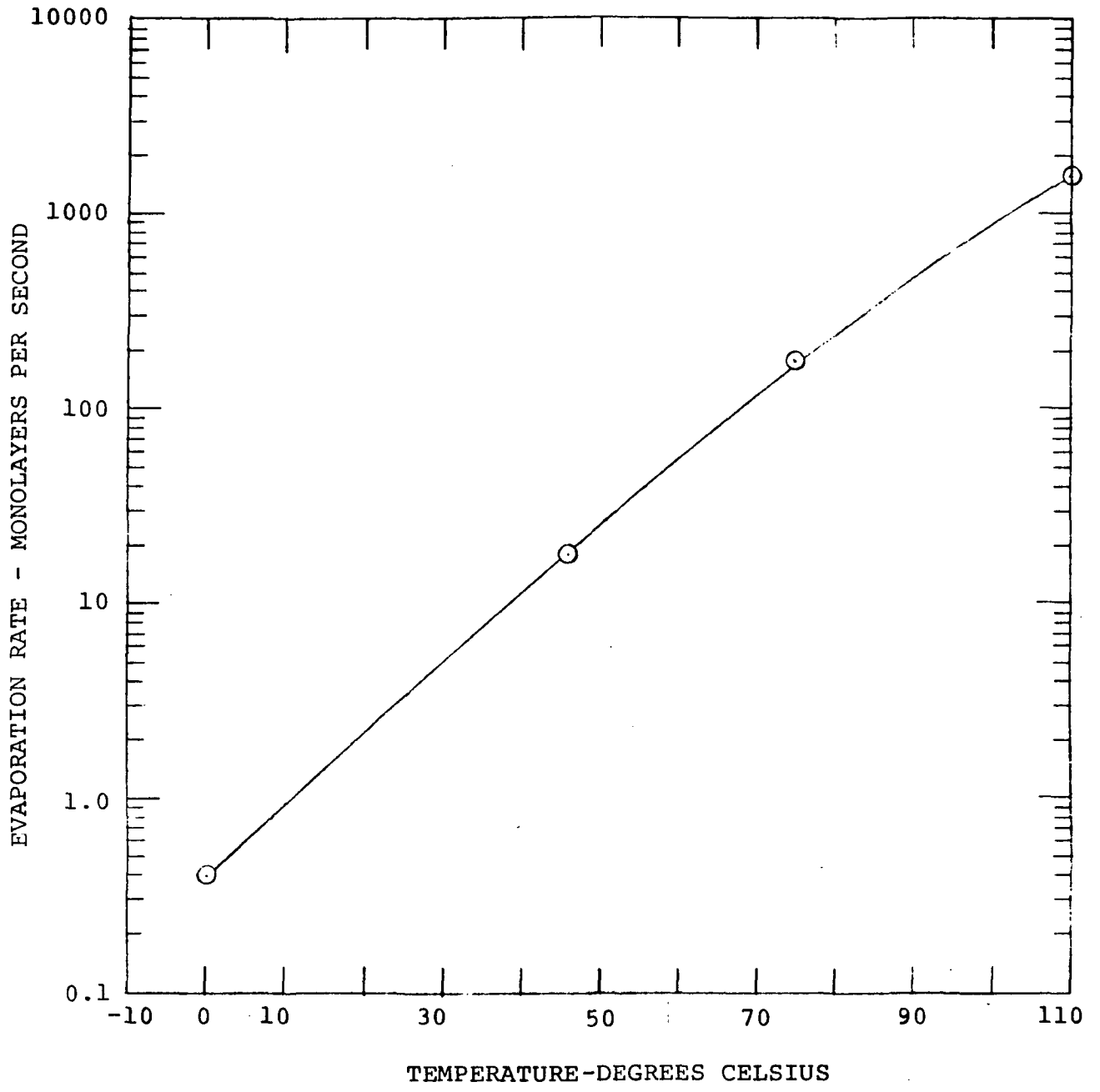
Figure 8. - Rate of Evaporation of Cesium Metal From
a Cesium Surface.
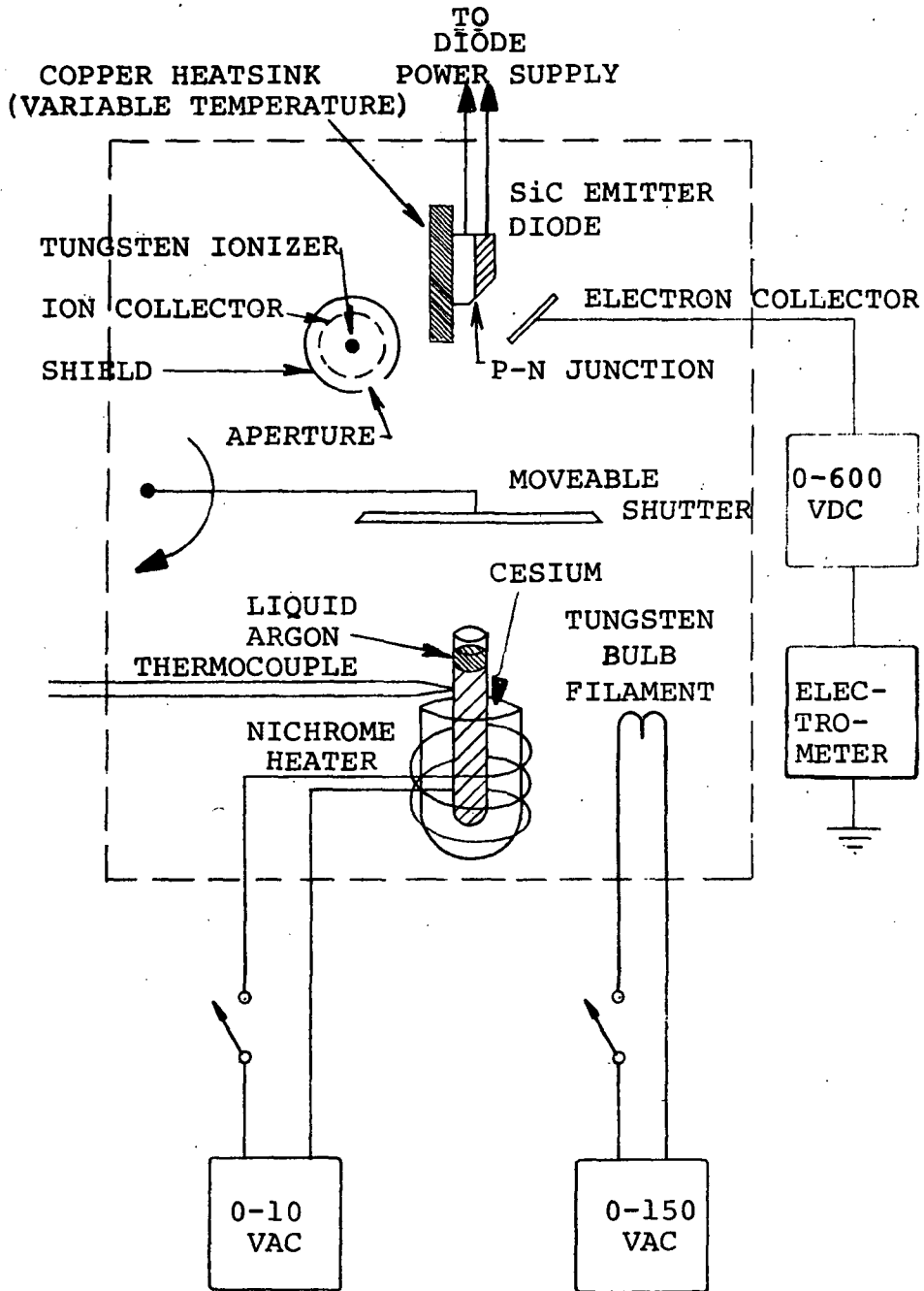
Figure 9. - Schematic of Cesium Deposition Experiment.

After installation of the cesium generation and detection apparatus shown in Figure 8 a search was made for a diode with greater than 10^{-8} A emission since that represents a current level 10 times the minimum level that may be detected with the pulsed diode scheme which must necessarily be used in order to limit the diode temperature as discussed above. Simultaneously with this the supply of diodes for testing was severely limited due to uncontrollable problems that had arisen in the operation of the SiC crystal pilot line. No diodes were found that could be used in testing the cesium deposition scheme with the exception of diode 3059-63-A3 and that device was required in the more necessary experiment to determine the effect of electron emission upon magnetron discharge gauge operation as will be discussed below.

ION IMPLANTATION

In recent years a group at Hughes Research Laboratories has successfully formed p-n junctions in SiC by means of ion implantation[13,14,15]. Since a junction formed in such a manner may be very close to the surface the possibility exists to obtain by this technique a large area for electron emission as opposed to the narrow junction width exposed at the crystal surface in the case of junction formation by epitaxial growth. In the latter case, those hot electrons generated within the bulk of the crytstal lose their energy interacting with photons and other electrons. The mean free path for the hot electrons was shown in reference 1 to be between 100 Å and 1000 Å depending on crystal perfection and hot electron energy.

It was assumed that if by ion implantation a p-n junction could be formed within a few hundred Angstrom units of the surface, enhanced electron emission would be observed because the accelerated electron would experience few, if any, collisions in their escape from the junction. Under the reasonable assumption that avalanche multiplications is the mechanism for the observed electron emission as opposed to Zener tunnelling, therefore lightly doped p type SiC crystals were desired. The transition of the breakdown mechanism from Zener tunnelling to avalanche breakdown as one proceeds from heavily doped Si to lightly doped has been shown by Chynoweth, et al.[11] The p crystals used in formation of the standard Norton junctions are heavily compensated, the starting material being relatively heavily nitrogen doped n material. Thus ion implantation into Norton material to form a shallow n layer would have to take place into p material with nearly .03% of acceptor impurities. No commercial source of lightly p-doped SiC was found. However, Westinghouse Corporation's Astronuclear Division agreed to supply some light doped p crystals upon NASA certification of the need for them in the electron emitter development program.

Arrangements were made with Sprague Electric Corporation to carry out nitrogen ion implantation into several of the p crystals, the doping levels of which were assumed to be between $10^{16}/cm^3$ and $10^{17}/cm^3$. The results of the ion implantation are shown in Table II and III which are the

TABLE II

SPRAGUE ELECTRIC COMPANY

Nitrogen in SiC

(Room Temp)

	$14\ N^{+}$ E (keV)	$14\ N^{+}$ D ($Ions/cm^2$)	$14\ N_2^{+}$ E (keV)	$14\ N_2^{+}$ D ($Ions/cm^2$)
1. 37-1 $x_j = 700\ \overset{\circ}{A}$			35	5×10^{14}
2. 37-2 $x_j = 1000\ \overset{\circ}{A}$	25	1×10^{15}	30	5×10^{14}
3. 37-3 $x_j = 1500\ \overset{\circ}{A}$	35	1×10^{15}	30	5×10^{14}
4. 40-1 $x_j = 1900\ \overset{\circ}{A}$	50	1×10^{15}	30	5×10^{14}
5. 40-2 $x_j = 2300\ \overset{\circ}{A}$	60	1×10^{15}	30	5×10^{14}
6. 40-3 $x_j = 2300\ \overset{\circ}{A}$	60 20	1×10^{15} 1×10^{15}		

C peak $\sim$ (1 - 3) $\times 10^{20}$ atoms/cm^3

C average $\sim$ 1 $\times 10^{20}$ for all implants

TABLE III

SPRAGUE ELECTRIC COMPANY

SiC Substrate

	ΔR_p (μM)	$^{14}N^+$ $R_p(\text{Å})$	at $1 \times 10^{15}/cm^2$ N peak	Å $\sim x_j$
60 keV	0.0306	1123	1.3×10^{20}	2300
50 keV	0.0268	931		1900
40 keV	0.0227	739		1700
30 keV	0.0182	550	2.2×10^{20}	1300
20 keV	0.0130	361	3.1×10^{20}	850
10 keV	0.0074	179	5.7×10^{20}	450
70 keV	0.0310	1313		2600
80 keV	0.0370	1500		3000
90 keV	0.0396	1674	1.0×10^{20}	3300

Want $\sim 10^{20}/cm^3$ $x_j = 3000, 2000, 1500, 1100, 800, 400$ Å

$$N \text{ peak} = \frac{10^4 C}{\sqrt{2\pi}(\Delta R_p)\mu M} \text{ atoms/cm}^3 \qquad\qquad \begin{array}{l} C = \text{Dose, ions/cm}^2 \\ \Delta R_p = \text{Standard deviation} \end{array}$$

$$= 4.0 \times 10^3 \frac{C}{(\Delta R_p)\mu M}$$

Ion Distribution: $\quad N/C = \dfrac{10^4}{(\Delta R_p)\sqrt{2\pi}} \exp \dfrac{(x - R_p)^2}{2(\Delta R_p)^2}$

$+ \ x_{junction} \doteq R_p + 4\Delta R_p$

reports received from Sprague, and the analysis leading to the determination of implanted range and profile following the work of Johnson and Gibbons "Projected Range Statistics in Semiconductors".[16] The page of interest from the latter is reproduced as Table IV.

At the same time preparations were made for measurement of the carrier concentration and the impurity type. An apparatus for carrying out 4-point probe resistivity and Hall effect measurements was constructed following the method of Van der Pauw[17]. Fortran IV computer programs were written to yield the carrier concentration, specific resistivity, carrier mobility, and Hall coefficient from the 4 point probe resistances, and the magnetic flux density. A listing of the computer programs is given in Appendix I. A cold probe was used to determine the major impurity type in classification of the crystals after implantation and subsequent annealing.

Numerous attempts were made to apply ohmic contacts to the Westinghouse material without success. Pure silver and tantalum-gold contacts which had been successfully used in measurements on Norton crystals did not provide ohmic contacts although the latter in general yielded reasonably low resistance contacts to the Westinghouse p material. A second problem in contacting the implanted junctions arises from the fact that the implanted layer which forms the junction lies extremely close to the surface. Any of the ohmic contacts that have been successfully made to SiC

TABLE IV

LSS RANGE STATISTICS FOR NITROGEN IN SILICON CARBIDE		ENERGY (KEV)	PROJECTED RANGE (MICRONS)	PROJECTED STANDARD DEVIATION (MICRONS)	RANGE (MICRONS)	STANDARD DEVIATION (MICRONS)	NUCLEAR ENERGY LOSS (KEV/MICRON)	ELECTRONIC ENERGY LOSS (KEV/MICRON)
SUBSTRATE PARAMETERS:		10	0.0179	0.0074	0.0269	0.0084	0.2819E 03	0.1232E 03
		20	0.0361	0.0130	0.0515	0.0147	0.2324E 03	0.1743E 03
SILICON	CARBIDE	30	0.0549	0.0182	0.0760	0.0200	0.1982E 03	0.2134E 03
		40	0.0739	0.0227	0.1001	0.0244	0.1725E 03	0.2465E 03
Z 14	6	50	0.0931	0.0268	0.1237	0.0282	0.1514E 03	0.2756E 03
		60	0.1123	0.0306	0.1469	0.0315	0.1355E 03	0.3019E 03
M 28.090	12.011	70	0.1313	0.0340	0.1694	0.0344	0.1250E 03	0.3260E 03
		80	0.1496	0.0370	0.1911	0.0368	0.1227E 03	0.3485E 03
N 0.4866E 23	0.4866E 23	90	0.1674	0.0396	0.2120	0.0389	0.1136E 03	0.3697E 03
RHO/P 0.1146E 02	0.4791E 02	100	0.1850	0.0421	0.2324	0.0408	0.1056E 03	0.3897E 03
		110	0.2024	0.0444	0.2524	0.0425	0.9859E 02	0.4087E 03
EPS/E 0.7201E-01	0.1356E 00	120	0.2195	0.0466	0.2719	0.0440	0.9267E 02	0.4269E 03
		130	0.2363	0.0497	0.2909	0.0454	0.8781E 02	0.4443E 03
CNSE 0.2320E 02	0.1577E 02	140	0.2529	0.0505	0.3095	0.0467	0.8401E 02	0.4611E 03
		150	0.2691	0.0523	0.3276	0.0479	0.8226E 02	0.4773E 03
MU 2.006	0.858	160	0.2850	0.0540	0.3453	0.0490	0.7890E 02	0.4929E 03
		170	0.3007	0.0555	0.3626	0.0500	0.7571E 02	0.5081E 03
GAMMA 0.8879	0.9942	180	0.3161	0.0569	0.3795	0.0509	0.7271E 02	0.5228E 03
		190	0.3312	0.0583	0.3962	0.0517	0.6988E 02	0.5372E 03
		200	0.3461	0.0596	0.4125	0.0525	0.6724E 02	0.5511E 03
		220	0.3753	0.0620	0.4443	0.0540	0.6248E 02	0.5780E 03
		240	0.4038	0.0642	0.4750	0.0553	0.5844E 02	0.6037E 03
		260	0.4314	0.0661	0.5047	0.0564	0.5512E 02	0.6284E 03
SND 0.2579E 03		280	0.4584	0.0679	0.5335	0.0575	0.5252E 02	0.6521E 03
		300	0.4847	0.0696	0.5615	0.0584	0.5030E 02	0.6750E 03
		320	0.5103	0.0711	0.5887	0.0592	0.4749E 02	0.6971E 03
ION: NITROGEN		340	0.5355	0.0725	0.6152	0.0600	0.4495E 02	0.7186E 03
		360	0.5601	0.0738	0.6411	0.0607	0.4266E 02	0.7394E 03
Z 7		380	0.5842	0.0750	0.6664	0.0614	0.4062E 02	0.7596E 03
		400	0.6078	0.0762	0.6911	0.0620	0.3881E 02	0.7794E 03
M 14.000		420	0.6310	0.0772	0.7153	0.0626	0.3724E 02	0.7986E 03
		440	0.6538	0.0782	0.7390	0.0631	0.3588E 02	0.8174E 03
		460	0.6761	0.0792	0.7622	0.0636	0.3475E 02	0.8358E 03
		480	0.6980	0.0800	0.7849	0.0641	0.3384E 02	0.8538E 03
		500	0.7196	0.0809	0.8072	0.0645	0.3314E 02	0.8714E 03
		550	0.7718	0.0828	0.8613	0.0655	0.3230E 02	0.9139E 03
		600	0.8218	0.0844	0.9130	0.0663	0.3046E 02	0.9545E 03
		650	0.8702	0.0859	0.9629	0.0671	0.2865E 02	0.9935E 03
		700	0.9169	0.0872	1.0109	0.0677	0.2706E 02	0.1031E 04
ELECTRONIC CROSS SECTIONS OF		750	0.9622	0.0884	1.0574	0.0683	0.2566E 02	0.1067E 04
LINDHARD, SCHARFF, SCHIOTT		800	1.0062	0.0895	1.1025	0.0688	0.2440E 02	0.1102E 04
		850	1.0489	0.0905	1.1462	0.0693	0.2328E 02	0.1136E 04
		900	1.0906	0.0914	1.1888	0.0698	0.2226E 02	0.1169E 04
		950	1.1312	0.0923	1.2302	0.0702	0.2134E 02	0.1201E 04
		1000	1.1708	0.0931	1.2706	0.0705	0.2049E 02	0.1232E 04

Reproduced from: Projected Range Statistics in Semiconductors
W. S. Johnson and J. F. Gibbens dist. by Stanford University Book
Store (1969). (Calculations based on L.S.S. Theory.)

have required diffusing-in or alloying the contact material with the SiC. The diffusion takes place over macroscopic distances of the material (e.g.,.1 mil thickness), so that the volume that is disturbed by making the contact is much thicker than an ion implanted junction would be (e.g., < 0.01 mil) and, thus, such a junction would be short-circuited.

Since the implanted (n) material is relatively highly doped, ($\approx 10^{20}/cm^3$) it may be that no difficulty would be had in obtaining a satisfactory ohmic contact without resorting to high temperature diffusion contact to it. The significant problem to be solved is that of obtaining ohmic contact to the lightly doped p material and thus knowledge of successful contact to the n material must come subsequent to the development of ohmic contacts to the p side material.

Following ion implantation, annealing of the junction is required to remove the damage done to the lattice by the action of the high energy ions implanted. The work done by Marsh et al.[13] at Hughes on the formation of pn junctions by ion implantation into SiC crystals showed that annealing at 1400°C for 2 minutes was required to obtain a reasonably large carrier concentration and electron mobility in such crystals. Annealing, in vacuum, of Westinghouse crystals ion-implanted at the Sprague Electric Corporation was carried out in the equipment shown schematically in Figure 10. The crystals were enclosed in capsules of platinum
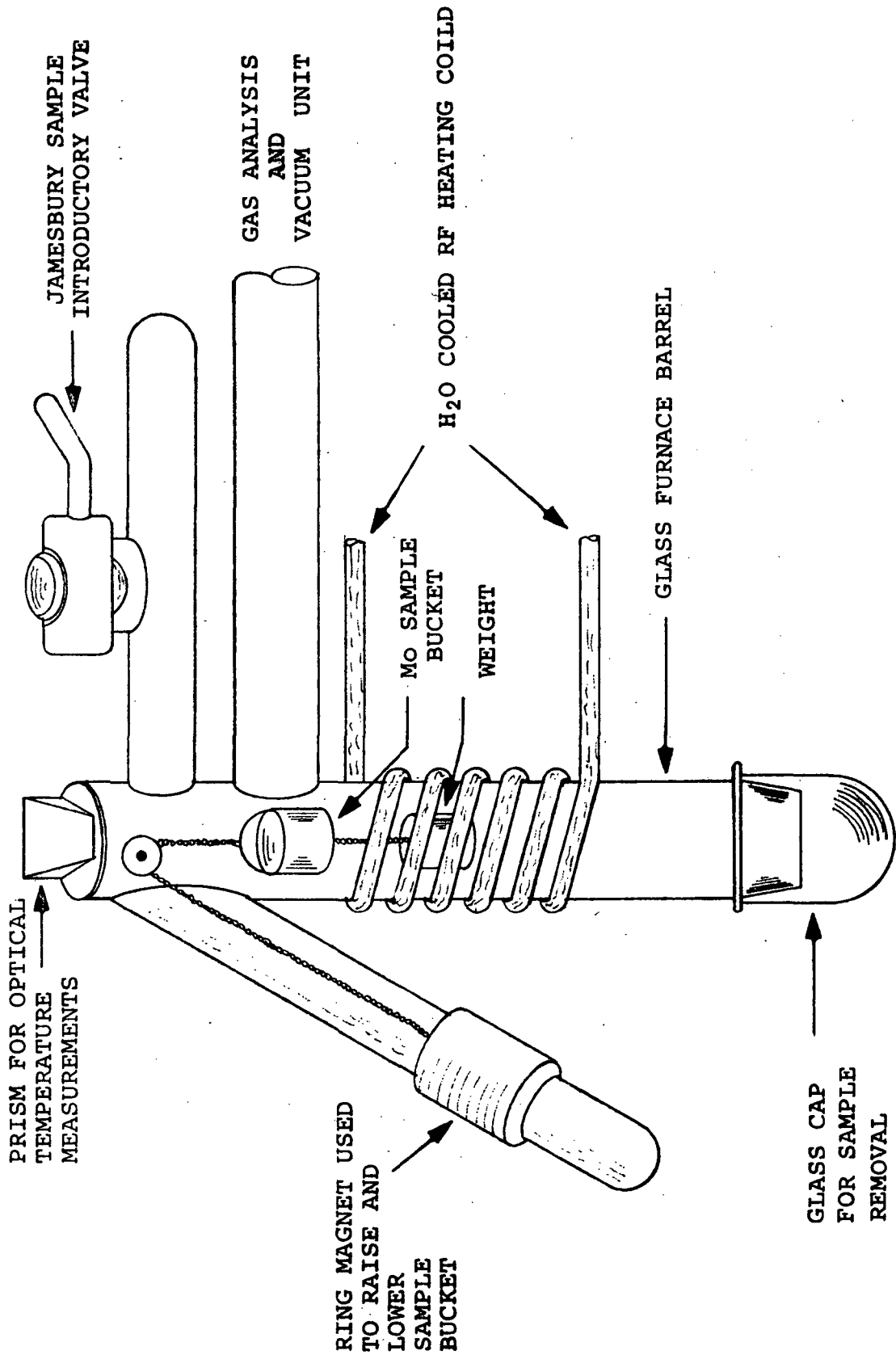
Figure 10. - Schematic of System for Annealing Ion Implanted SiC Crystals.

PRISM FOR OPTICAL
TEMPERATURE
MEASUREMENTS

RING MAGNET USED
TO RAISE AND
LOWER SAMPLE
BUCKET

JAMESBURY SAMPLE
INTRODUCTORY VALVE

GAS ANALYSIS
AND
VACUUM UNIT

H2O COOLED RF HEATING COILD

Mo SAMPLE
BUCKET

WEIGHT

GLASS FURNACE BARREL

GLASS CAP
FOR SAMPLE
REMOVAL

33

foil contained in the molybdenum sample bucket. Measurement of the Hall constant and resistivity of the resulting diode properties was attempted without success due to the lack of ohmic contact with the (lightly doped) p side of the diode.

Diamond Emitters

The generation of shallow p-n junctions to encourage large area emission of electrons need not be restricted to SiC crystals. If the reasonable assumption is made that the predominant mechanism for energy loss of hot carriers exiting the n region into vacuum is that of impact ionization then it may be shown that the material with the largest energy gap, E_g would have the highest probability of yielding high electron emission. It has been shown theoretically[18] that impact ionization requires an energy of about $3/2$ E_g and as long as this is greater than the electron affinity E_f, then hot carriers could exit the crystal. In the case of SiC, $3/2$ $E_g \approx 4.6$ eV and $E_f \approx 4.0$ eV so that conditions are faborable for electron emission. However, if one considered diamond with an energy gap of almost twice that of SiC it is immediately seen that excellent conditions for electron emission would exist in a p-n junction formed in such a materal. Diamond crystals are now available commercially in large enough sizes by the General Electric process. If the problem of ohmic contact to diamond p crystal can be solved the formation of diamond electron emitters using the technique of ion implantation should be investigated.

34

INITIATION AND LINEARIZATION OF MAGNETRON DISCHARGE

A secondary goal of the program was to use the p-n junction emitter as a cold cathode to supplement the discharge in a magnetron ion source. There are three important areas in which the p-n junction emitter could be useful in such gauges. First is in aiding the initiation of a magnetron discharge. The second area would be in the enhancement of linear discharge characteristics of the present Redhead magnetron. The third area for investigation would be in the development of a linear magnetron ion source with a sensitivity proportional to the p-n junction emitter current in the manner of the hot cathode magnetron gauge of Lafferty[18].

In the case of the initiation of a discharge in a normal magnetron gauge, depending upon the dimensions of the gauge and its electric and magnetic field strengths, there may be insufficient generation of secondary electrons at the optimum location for the discharge to build up to a stable one even though a discharge, once established, would maintain itself. The p-n junction emitter is used to introduce the required electron component. The location of introduction of these electrons is of great importance to their efficiency in aiding the initiation of the discharge and the smaller the number of such electrons needed for this initiation, the more desirable the use of such a source becomes. Once sufficient electrons

are added that the discharge becomes stable, generating
sufficient secondaries as a result of ionization of neutrals
and positive ion bombardment, then the initiating electron
emission may be ceased. In addition to its attraction of
requiring low power dissipation the use of a cold electron
emitter is desired in order to avoid the simultaneous
generation of gas which would mask the ambient gas concen-
tration to be measured.

A p-n junction emitter was placed nearly in the plane of
of one (grounded) cathode plate of an experimental magnetron
gauge as shown in Figure 11. The other cathode with its asso-
ciated axial rod was connected to an electrometer for purposes
of monitoring the presence of ions. The cylindrical anode was
operated at various voltages between 200 and 1000 volts dc. The
axial magnetic field was approximately 740 gauss. Figure 12
is a schematic of the experimental configuration. The meter
in the anode circuit is used in determining the emitted electron
current. The electric and magnetic field characteristics of the
particular magnetron gauge used were such that the gauge was
not self starting at pressures below about 6×10^{-6} Torr.

Figure 13 shows the effect upon the collected ion current
of increasing the emission current from the SiC p-n junction.
The behavior shown is independent of the presence of the magnetic
field. The dependence of I_e on impressed voltage is also
shown. Since the plotted voltage includes the temperature de-
pendent IR drop in the crystal in addition to the junction
voltage thus then there is anomalous behavior at higher voltage
where the crystal temperature is increasing. However, the
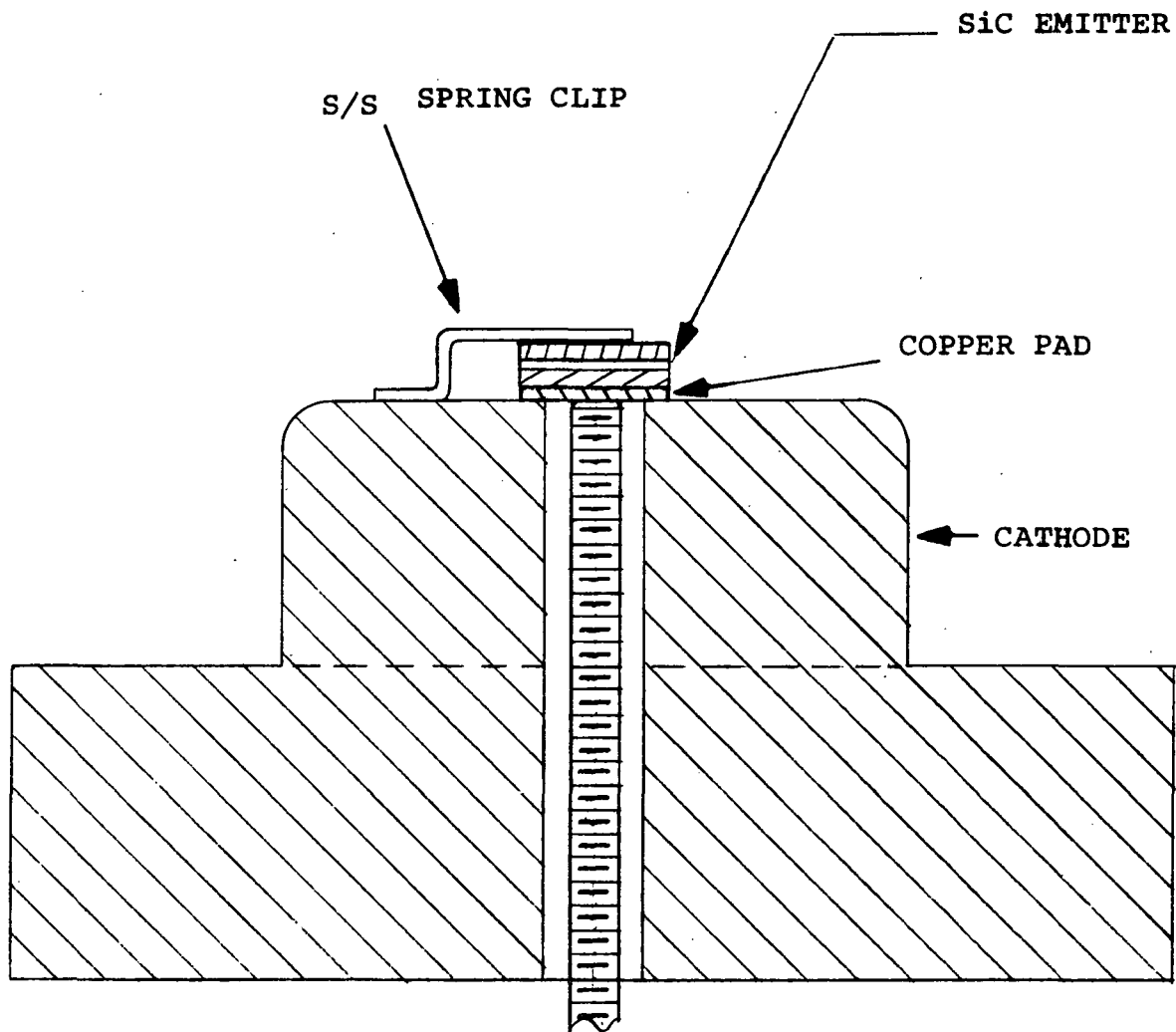threshold for emission at 12 volts is clearly visible.

Figure 11. - Schematic of Diode Mounting at Cathode of an Experimental Magnetron Ion Gauge.

ELEC-
TRO-
METER

ION CURRENT
DETECTION CATHODE

CYLINDRICAL
MAGNET

ANODE

SEE FIG. 11
FOR DETAIL

ELEC-
TRO-
METER

+

0-1000
VDC
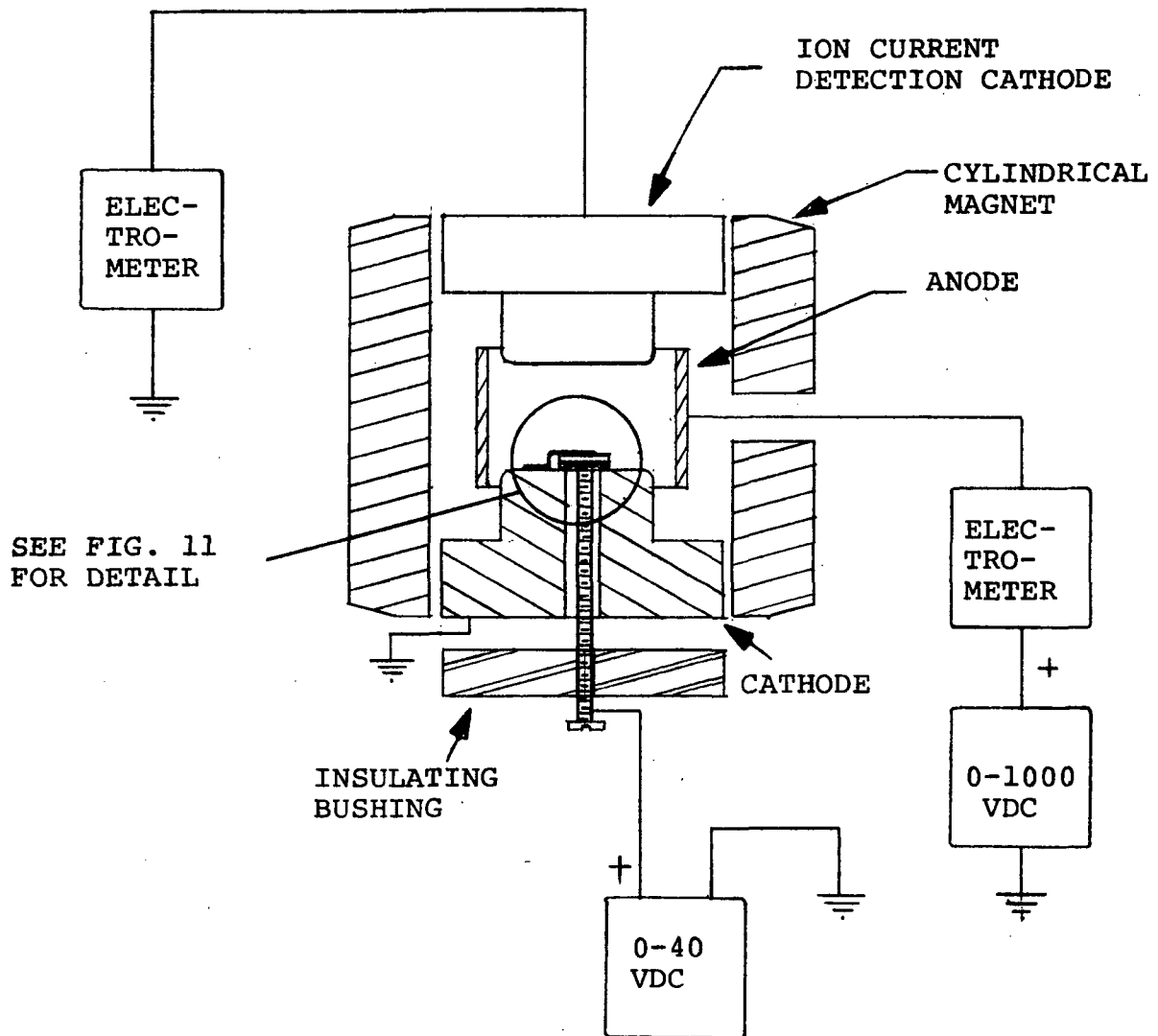
INSULATING
BUSHING

CATHODE

+

0-40
VDC

Figure 12. - Schematic of Experiment to Study Magnetron
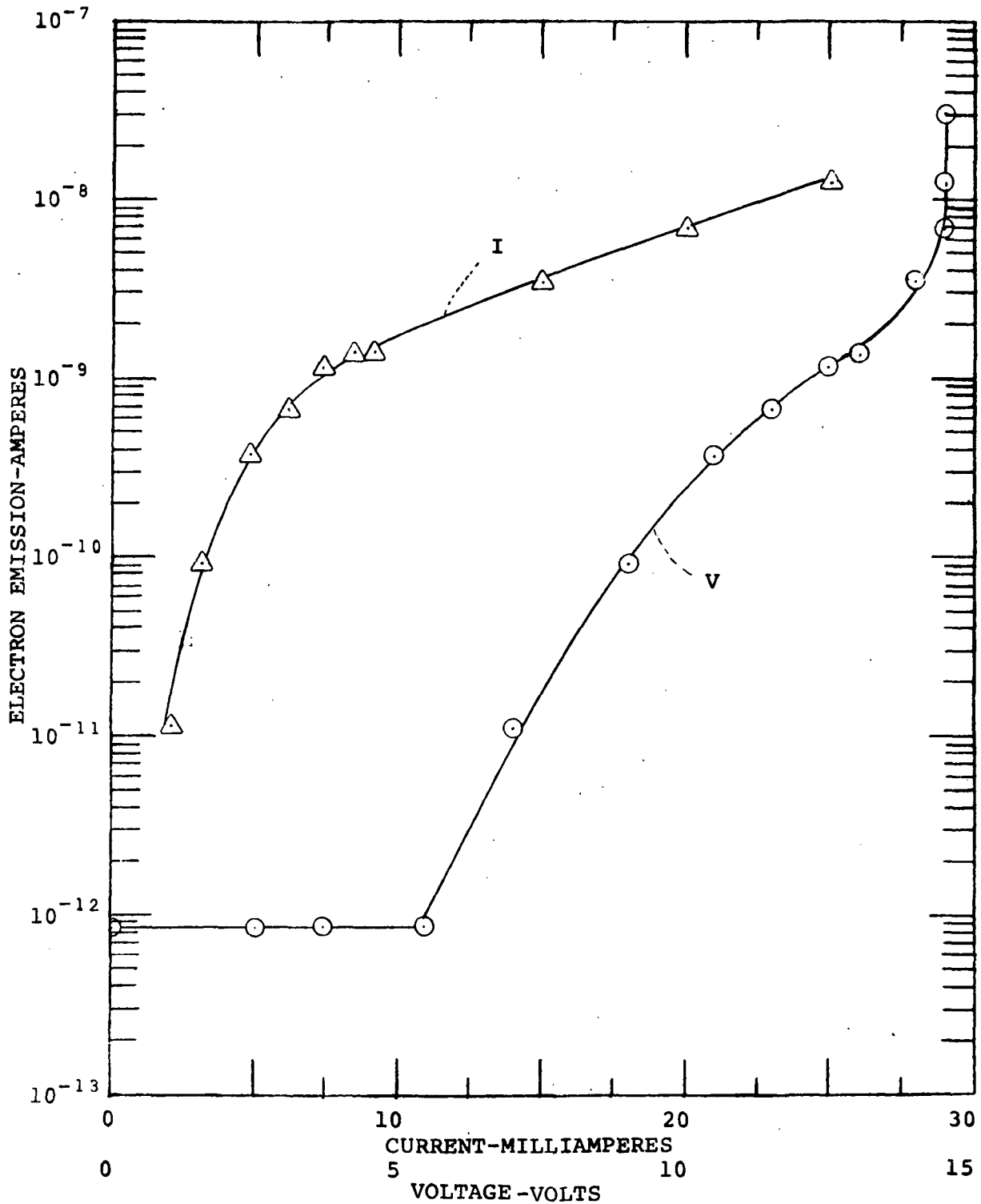Discharge Enhancement Using a SiC Electron
Emitter.

Figure 13. - Electron Emission Current vs. Junction Current
and Voltage for Diode 3059-63-A3.

Prior to the experiment it had been found that the electrons were coming from a region of the diode junction that was made visible by the usual electron-hole microplasma light emission. In mounting the diode, care was taken to place the emission site close (∿ 1 mm) to the anode in order that the maximum field be available to draw out the electrons. It is therefore unlikely that the ion current collected is due to primary ionization resulting from the directly emitted electron component since those ions would no doubt be collected at the grounded cathode where the emitter was situated. The ion current collected at the opposite cathode which was monitored is more probably predominantly that resulting from ionization by electrons resulting from secondary emission and is distributed throughout the volume of the anode-cathode space under the action of the crossed electric and magnetic fields. This resulting plasma represents the incipient conditions that subsequently results in a stable discharge once a threshold is reached such that the ion-electron pair generation rate is sufficient to compensate for the inherent loss rate for the device. Until enough electron current is emitted to encourage this sufficiency of pair generations, the removal of the emitted current component leads to complete decay of the plasma. Once the threshold is reached a stable self sustaining distribution of electrons is reached and decrease of the emitted current to zero does not lead to decay of the plasma below some level dependent on the device geometry
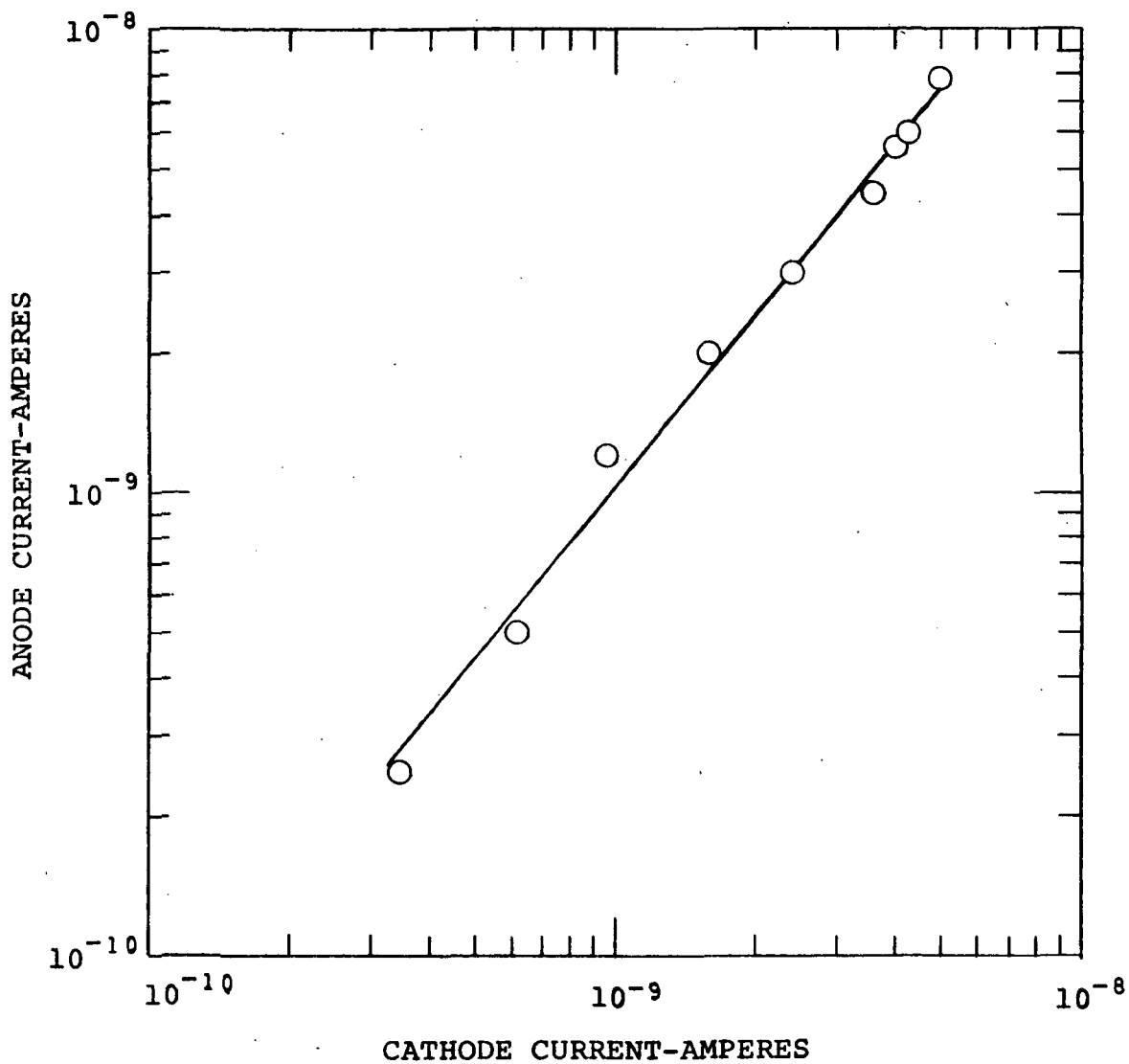
Figure 14. - Anode Current vs. Cathode Current for
the Experimental Ion Gauge with SiC Emitter.

and the electric and magnetic field distributions. This may be
seen in Figure 14 which shows the total cathode current which
is the sum of the collected ion current and the resulting
secondary emission versus the total anode current due to the
electrons collected there.

If the magnet is removed from the gauge the current
collected at the opposite cathode from that at which emission
takes place is more than 4 orders of magnitude smaller. The
electric field configuration in that case is apparently such
as to cause the collection of all ions at the emitting cathode.
The pressure in this case was approximately 6×10^{-7} Torr.
The discharge was not self sustaining without emission from
the diode since the ion current decayed to zero when the diode
junction current was ceased.

It is not altogether surprising that Figure 14 shows the
anode and cathode current are nearly linearly related since
the measurements made represent stable discharge conditions.
In such a case the total cathode current must be strictly equal
to the anode current and with the split cathode configuration
that exists in the experiment described the current collected
at one cathode will be some nearly constant proportion of the
total cathode current.

Since the discharge effectively masks the contributing
effect of the emitted electron current a series of experiments
were carried out to extract information on the relation of
emitter current to collected ion (plus secondary electron)
current. The measurement of emitter current collected at

the anode was made with the magnet removed from the gauge.
The magnet was then replaced and the ion current collected
at the cathode opposite the emitter was measured. An example
of such data is shown in Figure 15. It may be seen as
expected that since the discharge is nearly self starting
at this pressure then it requires but little emitted current
to initiate the discharge. Once the discharge occurs the
emitter current may be removed without effect. That condition
is shown by the solid circle in the Figure.

On the other hand if the pressure is reduced to about
10^{-7} Torr such that the stable discharge current corresponds
to less than the attainable emitter current an interesting
situation is found, an example of which is shown in Figure 16.
As before, their is a rapid increase of ion current with
emitted electron current until apparently a stable discharge
condition is attained at about 4.5 x 10^{-10}A. That is when
the emitter current has just exceeded the stable discharge
current with no emitter current (circled point). It appears that
at that point the introduction of electrons is sufficient to
overcome the loss mechanism for electrons, the discharge being
non self starting without this supply of electrons. However,
if the emission current is increased far above that value
corresponding to the stable conditions, the collected ion
current does not increase, but rather remains limited at the
value corresponding to the stable discharge conditions with no
cold emitted electrons. As the attempt is made to inject more
electrons into the discharge no increase in ion current is
observed. The solid circle indicates the anode-cathode current
conditions when the emitter current is decreased to zero.

Figure 15. - Cathode Current vs. Electron Current for the
Experimental Ion Gauge with SiC Emitter at
$\sim 10^{-6}$ Torr.

10^{-8}

10^{-9}

10^{-10}

10^{-11}

PRESSURE $\approx 10^{-7}$ TORR

ANODE VOLTAGE = 1KV

10^{-11} 10^{-10} 10^{-9} 10^{-8}

EMITTED CURRENT (MAGNET REMOVED) - AMPERES
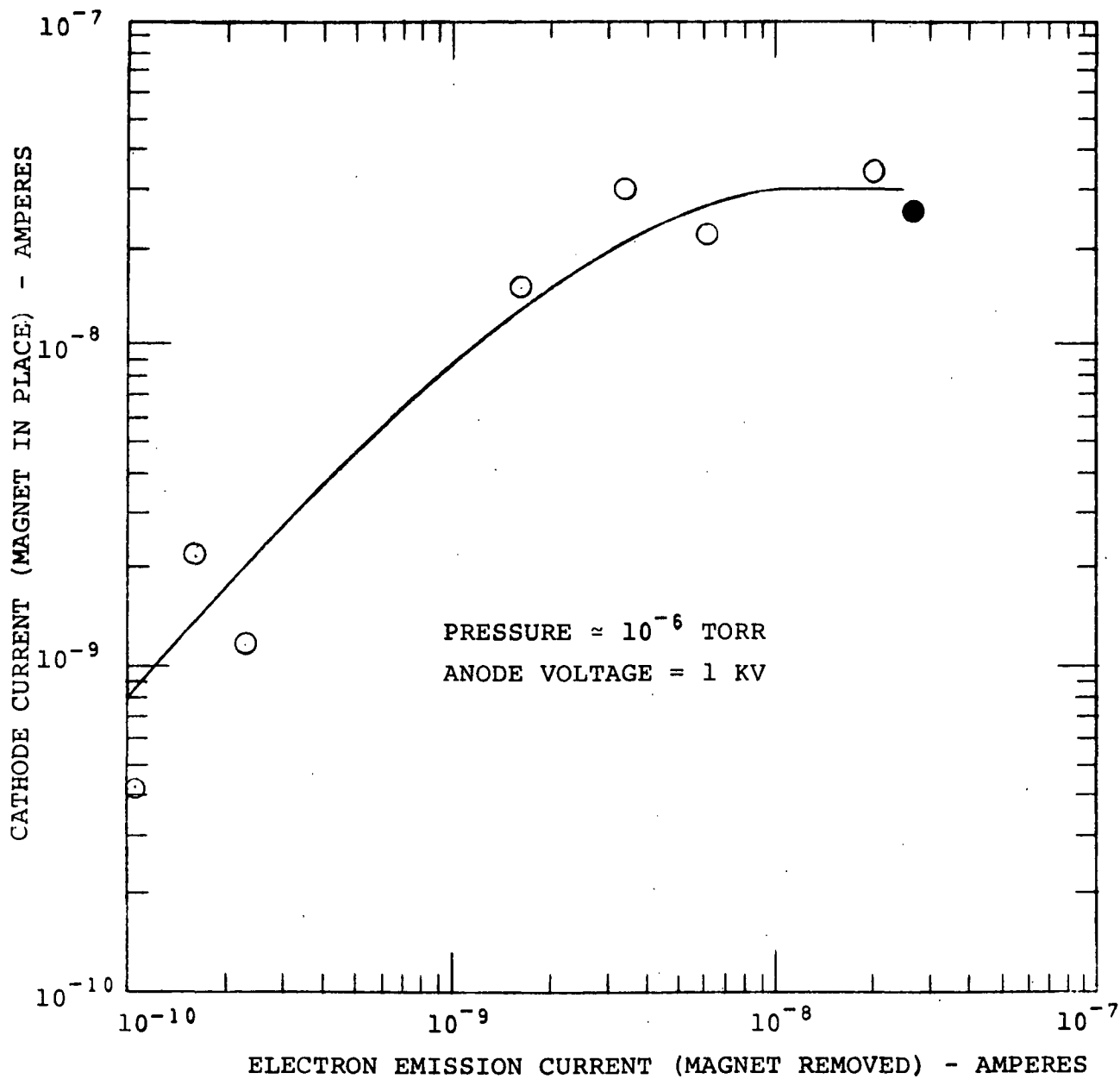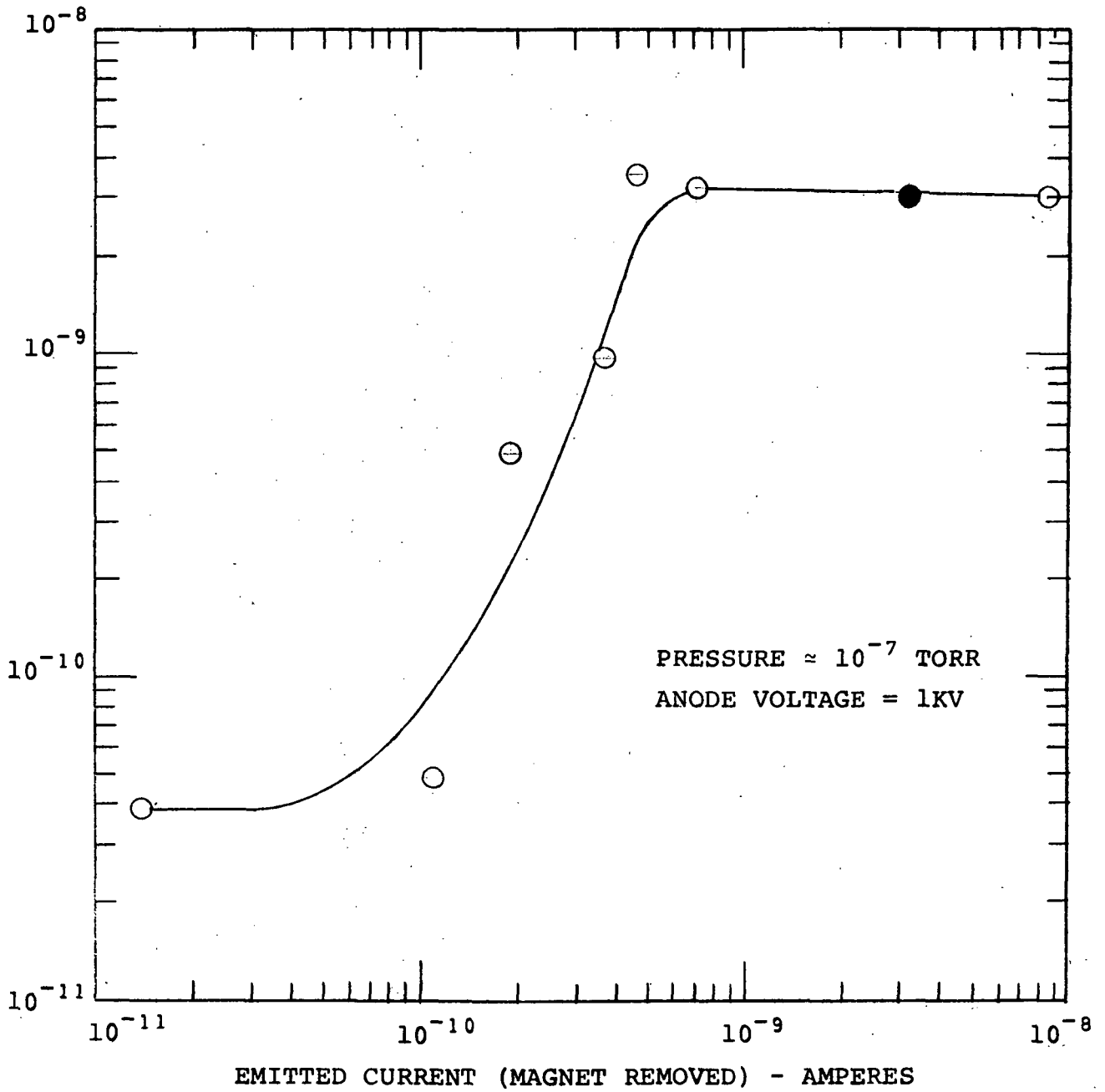
Figure 16. - Cathode Current vs. Emitted Electron Current for the Experimental Ion Gauge with SiC Emitter at $\sim 10^{-7}$ Torr.

45

There are two possible explanations of this behavior,
the least likely being that an attempt to increase the
density of electrons in the rotating electron cloud leads
in some manner to increased ion-electron recombination
to somehow balance the increased ionization due to the
additional electrons. More likely is the fact that the
effective ionizing current in the rotating electron cloud
resulting from the discharge is very much larger than the
emitted electron current. That this is so may be under-
stood if one assumes because of the increased electron path
in the magnetron gauge over that in the Bayard-Alpert gauge
structure that the gauge sensitivity, S, is increased by
as much as 10^3 to $\sim 10^4$ $Torr^{-1}$. (The magnetron structure
of Lafferty[18] attained a sensitivity greater than that).
With this assumption the effective ionizing current for the
gauge would be approximately

$$I_- = \frac{I+}{pS} \quad .$$

Thus for $I_+ = 3 \times 10^{-9}$ A as observed and $p = 10^{-7}$ Torr
then

$$I_- = 3 \times 10^{-6} \text{ A.}$$

The maximum emitted current was 8.5×10^{-9} A and is
thus negligible compared with the probable effective ionizing
electron current in the gauge and as observed, should have
had no measurable effect on the collected ion current.

It follows from these considerations that the effect
of an emitter in a Redhead gauge will have little effect
on the ion current unless the emitted current is much
greater than the ion current and in fact the case investigated
the required emitter current is on the order of the maximum
current that has been observed from SiC diodes. For the
normal Redhead gauge which has a current sensitivity more than
an order of magnitude larger than the experimental gauge used
(4A/Torr vs. 0.1A/Torr) the emitted current required would
be at least 10^{-5}A. Since the maximum observed diode
efficiency is on the order of 10^{-5} thus the junction current
required would be at least 1 ampere and for such currents
the device may not be run under dc conditions because of
excessive power dissipated (> 10 wt) at such a current.
Thus, the one benefit to be gained from the use of a SiC
electron emitter in a Redhead magnetron is its ability to
initiate a discharge which would not otherwise commence.
The current required for that initiation appears to be about
equal to the gauge ion current for the pressure of interest.

On the other hand the third area in which the SiC p-n
junction emitter could be useful, namely its' use in place
of the hot cathode of a Lafferty magnetron gauge has great
possibilities because of its low temperature which would
lead to little interference by generating or dissociating
gases in the gauge. In addition, the emission current re-
quired for linear operation (< 10^{-7} A) is well within the
normal range of output of many SiC diodes.

REFERENCES

1. Oman, R.: Research and Development Program to Produce a *Silicon Carbide Cold Cathode (Hot Electron) Emitter*. NASA CR-66796, 1968.

2. Patrick, L.; and Choyke, W. J., Phys. Rev. Let. 2, 48 (1959).

3. Stepanov, G. V., Pokalyakin, V. I., and Elinson, M.I., Sov. Phys. - Sol. St. 3, 1280 (1961).

4. Brander, R. W. and Todkill, A. Mat. Res. Bull. 4, S305 (1969).

5. Bellau, R. V., Brander, R. W., Sutton, R. P., and Todkill, A., The General Electric Ci. Ltd., Central Research Laboratories, Sept. No. 15025C, 23 Nov. 1967, p. 7 (AD 826514).

6. Greebe, C. A. A. J., Phil. Res. Repts. Suppl. 1 (1963), p. 33.

7. Brander, R. W. Todkill A., Mat. Res. Bull. 4, S309 (1969).

8. Patrick, L. and Choyke, W. J., Phys. Rev. Let. 2, 49 (1959).

9. Hodgkinson, R. J., Brit. J. Appl. Phys. 15, 1483 (1964).

10. Windsor, E. E., Vacuum 20, 7 (1970).

11. Chynoweth, A. G., Feldmann, W. L., Lee, C. A., Logan, R. A., and Pearson, G. L., Phys. Rev. 118, 425 (1960).

12. Brander, R. W., and Todkill, A., Mat. Res. Bull. 4, S308 (1969).

13. Marsh, O. J.; Hunsperger, R. G.; Dunlap, H. L.; and
    Mayer, J. W.: Development of Ion Implantation Techniques
    for Microelectronics. NASA CR-86014, 1967.

14. Hunsperger, R. G.; Dunlap, H. L.; and Marsh, O. J.:
    Ion Implantation Techniques for Microelectronics.
    NASA CR-86142, 1968.

15. Dunlop, H. L. and Marsh, O. J., Appl. Phys. Let. 15, 311
    (1969).

16. Johnson, W. S. and Gibbons, J. F., Projected Range
    Statistics in Semiconductors, dist. by Stanford University
    Book Store (1969).

17. Van der Pauw, L. J., Phil. Res. Rpts. 13, 1 (1958).

18. Wolff, P. A., Phys. Rev. 95, 1415 (1954).

Page Intentionally Left Blank

APPENDIX I

FORTRAN PROGRAMS FOR ANALYSIS
OF 4 POINT PROBE HALL EFFECT MEASUREMENTS

MAIN PROGRAM HALL 4

```
            TYPE 500
            ACCEPT 100, THE
11          TYPE 200
            ACCEPT 100, R1
            TYPE 300
            ACCEPT 100, R2
            TYPE 400
            ACCEPT 100, RDFL
            TYPE 930
            ACCEPT 100, RZ
            RZ=(R1-R2)/(B1+B2)
            R=R1/R2
            T=TH*. 00254
            X=1.
               DX=1.
10          Y2=RZ-F(X)
            IF(Y2)3,2,5
5           IF(Y2-.001)2,2,1
1           DX=DX/2
            X=X-DX
            GO TO 10
3           IF(Y2+.001)4,2,2
4           DX=DX/2
            X=X+DX
            GO TO 10
2           TYPE 100,X
            TYPE 100,R
100         FORMAT(E)
200         FORMAT( ' R1LG ')
300         FORMAT( ' R2SM ')
```

51

```
                    XRES=2.27*T*(R1+R2)*X
                    TYPE 900
                    TYPE 600,XRES
                    RH=RDEL*T*2,*10000.
                    TYPE 700
                    TYPE 600, RH
                    XMOB=RH/XRES
                    TYPE 910
                    TYPE 600,XMOB
                    XCC=10.**19/(1.6*RH)
                    TYPE 800
                    TYPE 100,XCC
                    XN2=XCC/10.**16
                    TYPE 92N
                    TYPE 600,XN2
                    XC=(5.*(XT-32.))/9.
                    XK=1./(273.+XC)
                    TYPE 940
                    TYPE 600,XK
              400   FORMAT( ' RDEL ')
              500   FORMAT( ' TH ')
              600   FORMAT(F)
              700   FORMAT( ' RH ')
              800   FORMAT( ' XCC ')
              900   FORMAT( ' XRES ')
              910   FORMAT( ' XMOR ')
              920   FORMAT( ' XN2 ')
              930   FORMAT( ' TEM.F ')
              940   FORMAT( ' I/K ')
```

```
950       FORMAT( ' T.K ')
          XIK=273.+XC
          TYPE 950
          TYPE 600, XTK
          GO TO 11
          END
```

FUNCTION SUBROUTINE FUNCT

```
FUNCTION F(Y)
D={EXP((ALOG(2.))/Y))/2.
F=Y/ALOG(2.)*ALOG(D+SQRT(D*D-1.))
RETURN
END
```